NBSIR 74-572

Torsional Buckling of Composite Cylindrical Shells

D. E. Marlowe and G. F. Sushinsky

Engineering Mechanics Section
Mechanics Division
Institute for Basic Standards
National Bureau of Standards
Washington, D. C. 20234

September 1974

Final

Prepared for
National Aeronautics and Space Administration
Langley Research Center
Hampton, Virginia 23365

NBSIR 74-572

TORSIONAL BUCKLING OF COMPOSITE CYLINDRICAL SHELLS

D. E. Marlowe and G. F. Sushinsky

Engineering Mechanics Section
Mechanics Division
Institute for Basic Standards
National Bureau of Standards
Washington, D. C. 20234

September 1974

Final

Prepared for
National Aeronautics and Space Administration
Langley Research Center
Hampton, Virginia 23365

U. S. DEPARTMENT OF COMMERCE, Frederick B. Dent, Secretary
NATIONAL BUREAU OF STANDARDS, Richard W. Roberts, Director

CONTENTS

of these materials in complex structures requires a thorough knowledge of the behavior of these materials when subjected to various mechanical loadings. Considerable data already exist on the tensile and compressive behavior of these materials, whereas shear data are not abundant. The need for shear data prompted experimental investigations (refs. 3 and 4) of the torsional behavior of thin-walled cylindrical shells laminated with unidirectional composites and aluminum cylindrical shells reinforced with unidirectional composites.

The primary purpose of the investigation reported herein was to investigate the elastic torsional buckling strength of all-composite and composite-reinforced metal shells in which the composite laminate is not unidirectional. Test results on 39 specimens are reported. Boron/epoxy composite specimens in three lengths and two diameters, and graphite/epoxy composite specimens in two lengths and two diameters were tested. In addition, three configurations of composite-reinforced-aluminum-alloy and titanium-alloy specimens were studied. The effects of stacking sequence, direction of loading, and linear scaling of specimen dimensions were studied and an investigation of a stronger or "more optimum" stacking sequence was analytically determined and subsequently investigated experimentally.

This investigation was conducted at the National Bureau of Standards under the sponsorship and with the financial assistance of the National Aeronautics and Space Administration, Langley Research Center.

2. NOMENCLATURE

2.1 Units

The units for physical quantities used in this report are given in both the U. S. Customary Units and the International System of Units (SI). Measurements and calculations were made in U. S. Customary Units. Conversion factors relating the two systems are presented in Appendix A3 of reference 5.

2.2 Designations

The system for designating specimens which identifies both the specimen material and the specimen length is given in table 1. In the following tables a sample number is appended to this designation.

The stacking sequence or ply orientation for a laminate is designated by $(\alpha_1, \alpha_2, \alpha_3, --)_s$ where the α_1 is the ply angle of the outermost lamina, α_2 is the ply angle of the second lamina, etc. The subscript "s" indicates cases where the stacking sequence is symmetric about the mid-thickness of the shell. Positive ply angle is measured clockwise from a generator line on the cylindrical surface as shown in figure 1.

3. ANALYSIS

3.1 Torsional Buckling

The computer program "Buckling of Generally Orthotropic Cylinders," which was developed by Chao (ref. 6), was used to predict the buckling torques for each specimen. These were compared with the experimental results. In the program, buckling loads are calculated for a multi-layered cylindrical specimen loaded in combinations of torsion, axial compression and radial pressure. Chao's theory treats orthotropic layers of composite material whose principal material axes can be oriented in any direction. Specimen buckling is analyzed using Timoshenko's general equations of equilibrium (ref. 7). Using the concept of reduced flexural rigidity, the bending and membrane forces are uncoupled. The specimen is then assumed to have orthotropic elastic properties. The program seeks the solution with the lowest buckling torque by iterating on the number of circumferential buckling waves.

3.2 Design of an Optimum Laminate

Wu investigated the torsional buckling strength of all-composite four-ply cylindrical shells using two specific stacking sequences (ref. 8, fig. 27). Using this as a point of departure, several similar curves were produced using the Chao analysis in an effort to determine an "optimum" four-ply laminate configuration for both all-composite and composite-reinforced-metal cylinders. A comparison of some of these curves, including the stacking sequences chosen by Wu*, is shown in figure 2. Similar curves for boron/epoxy-reinforced-titanium cylinders are shown in figure 3.

4. SPECIMENS

The experimental program consisted of room-temperature torsional testing of 39 cylindrical shells designed to fail by elastic torsional buckling. Replicate samples were tested for each specimen configuration. Table 2 presents the geometry, laminate thicknesses, filament volume fractions, and stacking sequence for each of the individual specimens. Composite specimens were tested in three lengths and two diameters, and reinforced-metal specimens were

---

*The buckling torques of these stacking sequences are computed for a negative loading according to Chao's sign convention.

tested in one length and one diameter. The dimensions for the all-composite specimens wese chosen such that two diameter-to-thickness (D/t) ratios and three length-to-radius (L/r) ratios were tested.

4.1 Composite Materials

The boron/epoxy material used in this investigation was purchased in 3.0-in (7.6-cm) wide tape. The tape contained 0.004-in (0.01-cm) diameter filaments pre-impregnated with a 350 °F (180 °C)-curing epoxy resin system. This material was supplied with a 0.001-in (0.003-cm) fiberglass scrim cloth to facilitate handling.

The graphite/epoxy material used was a high-modulus graphite fiber pre-impregnated with a 350 °F (180 °C)-curing epoxy resin system. The pre-impregnated material was supplied by the manufacturer in the form of 3.0-in (7.6-cm) wide tape.

All uncured resin materials were stored at 0 °F (-18 °C) prior to use.

4.2 Composite-Reinforced-Aluminum-Alloy Specimens

The aluminum-alloy cylinders, which were to be reinforced with composite material, were machined from a single lot of 6061-T6 seamless drawn tubing. These cylinders had a nominal wall thickness of 0.022 in (0.056 cm) and a nominal outer diameter of 6.0 in (15 cm). The specimens tested had a gage length of 10.0 in (25.4 cm). The thickness of the composite reinforcement was approximately equal to the thickness of the aluminum-alloy cylinder. The dimensions of these specimens are shown in table 2.

4.3 Composite-Reinforced-Titanium-Alloy Specimens

The titanium-alloy cylinders, which were to be reinforced with composite material, were rolled from 6Al-4V titanium-alloy sheet and butt welded along the seam. The finished cylinders had a nominal wall thickness of 0.025 in (0.064 cm), a nominal outer diameter of 6.0 in (15 cm), and a gage length of 10.0 in (25.4 cm). The dimensions of these specimens are shown in table 2.

4.4 Material Properties

Longitudinal elastic modulus (E_{11}), transverse elastic modulus (E_{12}) and Poisson's ratio (ν_{12}) were determined for all materials used in this program. The preparation of and testing procedure for these specimens are described in the appendix to reference 3. The in-plane shear modulus (G_{12}) was determined for each material as the average value obtained from torsional tests on the 0-degree unidirectional composite specimens and the all-metal specimens tested in this program and in the program reported in refs. 3 and 4. The average material properties measured on the aluminum-alloy, titanium-alloy, boron/epoxy, and graphite/epoxy materials are shown in table 3.

The values of elastic moduli for the composite materials, E_{11}, E_{12}, and G_{12}, were corrected for thickness variation when they were used in the analysis. A rule-of-mixtures equation,

$$E_k = \frac{t_c E_c + (t_k - t_c) E_m}{t_k}$$

was used where

E_k = the corrected modulus,

t_c = nominal thickness of the composite,

t_k = measured thickness of the composite,

E_c = measured modulus of the composite,

and E_m = nominal modulus of the epoxy matrix material.

4.5 Specimen Fabrication

Boron/epoxy and graphite/epoxy-composite cylinders were fabricated in a manner similar to that described in refs. 3 and 9. The composite material was laid-up over a mandrel and covered by one ply of treated release cloth and the number of fiberglass bleeder plies required to absorb the excess of epoxy resin from the curing sample. Pressure was applied by enclosing the layup in FEP heat-shrinkable fluorocarbon tubing. A thermocouple was embedded in the laminate and the specimen was cured using the manufacturer's suggested time-temperature cycle.

The aluminum-alloy and titanium-alloy cylinders which were reinforced on the outer surface with composites were chemically cleaned and primed immediately prior to the layup process. A single layer of film-epoxy adhesive was applied to the metal cylinder followed by the required number of plies of prepreg material, glass release cloth, bleeder, and heat-shrinkable tubing. With the boron/epoxy prepreg, it was necessary to add an additional layer of 0.001-in (0.003-cm) fiberglass scrim cloth between the film-epoxy adhesive and the first ply of boron/epoxy in order to balance the total laminate. The composite layup techniques for these cylinders were similar to those used for the all-composite specimens, except that the metal cylinder served as a non-removable mandrel.

5. TESTING PROCEDURE

5.1 Instrumentation

Each of the cylindrical test specimens was instrumented on the outer surface of the shell at the midlength. Five 45° rosette foil strain gages having a gage length of 0.25 in (0.63 cm) were equally spaced around the specimens. These were oriented to measure strains in the axial direction and at ±45° to the axial direction. Several specimens were tested with additional strain gages in an attempt to detect the earliest indication of buckling and to check the uniformity of strain distribution.

5.2 End Fixtures

The end fixtures used for the all-composite specimens are shown in figure 4a. They are close-fitting end plugs which are bonded to the inner surface of the cylinder with an epoxy adhesive. The end fixtures used to test the composite-reinforced-metal specimens are shown in figure 4b. In these fixtures, both the inner and outer surfaces of the cylinders are bonded into the end fixtures.

5.3 Torsional Testing Procedure

Thirty-three specimens were tested in the Engineering Mechanics Laboratory of the National Bureau of Standards in a 40,000-lbf-in (4,500-N-m) capacity torsional testing machine (ref. 10). Six other specimens were tested at the NASA-Langley Research Center, Structures and Materials Laboratory. These included two 40-in (101.6-cm) long all-composite specimens tested in a 60,000-lbf-in (6,800-N-m) capacity torsional testing machine and four composite-reinforced metal specimens tested in torsion in a 100,000-lbf-in (11,300-N-m) capacity triaxial testing machine. A typical test setup in each of these machines is shown in figure 6. Torque was transmitted from the testing machine heads to the specimen fixtures by means of rectangular keys inserted through slots in the testing machine heads and the specimen end fixtures. All tests were performed at room temperature and at a uniform twisting rate of 0.005 rad/min.

During the torsional tests performed at the National Bureau of Standards, strain measurements were made at discrete values of torque. The magnitude of the torque increment between successive sets of strain readings was determined by the specimen behavior during the previous increment. During tests performed at the NASA-Langley Research Center, torque and strain were recorded at a virtually continuous rate in NASA-Langley's central digital-data recording facility.

All specimens were first loaded with a negative (counterclockwise) torque (fig. 1). This direction of twist caused a tensile stress in the filaments of cylinders fabricated with positive ply-orientation angles. Several specimens were loaded in both the positive and negative directions to determine the effects of the direction of twist on the buckling strength.

6. TEST RESULTS

6.1 Elastic Behavior of Specimens

The elastic properties of the torsional specimens tested are shown in table 4. This table gives the effective values of E_{11} and G_{12} which were predicted by the laminate analysis of the Chao program and measured during tests. The experimental moduli were determined from a least squares fit to the data of the first six load increments applied in the linear elastic range of each test.

6.2 Shear Stress-Shear Strain Curves

The shear stress-shear strain curves from all specimens tested are shown in figure 7. The shear strains were averaged from the measurements made at the mid-length of the specimens with the five rosette gages. Curves for aluminum-alloy specimens similar to the 20-in (50.8-cm) specimjns reported here are given in reference 3.

6.3 Buckling Torque

The maximum measured torques for the specimens tested in this investigation are given in table 5. These represent experimental buckling torques except where noted. Included in this table are the values of the buckling torque predicted by the Chao analysis and the ratio (correlation factor) of the maximum measured torque to the torque predicted by the analysis. The elastic material properties used in the analysis to predict the buckling torques are those presented in table 3 corrected for thickness variations.

Photographs of typical buckled specimens are shown in figure 8.

7. DISCUSSION

7.1 Elastic Buckling

The ability of the Chao theory to predict the buckling load of composite cylinders loaded in torsion can be estimated by analysis of the data given in table 5. For the specimens which fail by elastic buckling, the correlation factor between analysis and experiment is .81 with a standard deviation of 13 percent. This is approximately the same degree of agreement as that generally attributed to Donnell's treatment of isotropic cylinders (ref. 11). It is interesting to note that the analysis appears to be in better agreement with experiments for boron/epoxy specimens than for graphite/epoxy specimens. An evaluation of the effects of fabrication variables can be made by comparing the measured buckling torques of replicate specimens. The standard deviation of the differences in measured buckling torques between replicate specimens was five percent for all specimens tested which failed elastically. The difference between 13 percent and 5 percent reflects the "modeling error" in using the prediction equation. There appears to be a tendency for higher strength specimens fo fail by mechanisms other than elastic buckling.

7.2 Effect of Direction of Twist

The effect of direction of twist in specimens with unidirectional, off-axis layups is shown by the results on specimens BL03, (ref. 4, Table 4) BL05, BL06 and BL07 (table 5). Specimens BL03 (Predicted Buckling Torque, 3,480 lbf-in (393 N-m), Experimental Buckling Torque 3,400 lbf-in (384 N-m)) and BL07 with the +45-degree ply orientation failed by elastic buckling near the predicted value. However, the two specimens with -45-degree orientation, where principle tensile stresses were normal to the fibers, failed in the matrix or matrixfiber interface at torques well below the expected elastic buckling torques.

A more complete understanding of the effects of direction of twist and stacking sequence is obtained from the behavior of specimens B01 through B04 and C04, C06, C07 and C08. These specimens were symmetric, balanced ±45-degree laminates. They were twisted in both the positive and negative directions. In all cases, the direction of twist which loaded the outer ply fibers in compression resulted in the higher buckling torques (figs. 9 and 10). In general, these torques were approximately twice the torques of the specimens twisted in the direction in which the fibers in the outer ply were loaded in tension.

7.3 Linear Scaling

The effect of a linear scaling of cylinder dimensions was examined. Specimens B05 and B06 were half as long, half as thick and had one-half the diameter of specimens BL08 and BL09. This scaling resulted in the same L/r and D/t ratios. As predicted by the analysis, and as can be seen in table 6, the buckling shear stresses for the two sizes tested are nearly equal for both sizes of cylinder (fig. 11). Similar results were expected on specimen pairs C09, C10 and CL01, CL02. However, specimens CL01 and CL02 failed at loads well below the expected buckling torques. These failures were catastrophic without evidence of prior buckling. These premature failures may have been caused by local irregularities in the cylinder wall. Such irregularities could have occurred during the fabrication of the shell.

Specimens were also tested in which the effect of scaling only the specimen length was examined (fig. 12). These specimens were fabricated with a nominal 6-in (15-cm) diameter and 4 ply laminate thickness in three lengths. As can be seen from table 2, specimens B01 and B02 were 10 in (25.4 cm) long, specimens BL10 and BL11 were 20 in (50.8 cm) long, while specimens BLL01 and BLL02 were 40 in (101.6 cm) long.

7.4 Optimum Layup

Using the results of the computer study shown in figure 2, specimens were fabricated and tested with a stacking sequence of (-82.5, 30, 20, -82.5) degrees. As predicted by the analysis and as can be seen in table 7, the buckling torque for the optimum layup is twice that for a $(-45, +45)_s$ degree layup and seven times the buckling torque for a $(0,0)_s$ degree layup.

7.5 Composite-Reinforced-Metal Specimens

Tests were performed on specimens in which composite reinforcement, in accordance with the "optimum" ply stacking sequence discussed above, had been applied to the outer surface of thin-walled metal cylinders. This was a further evaluation of a concept for the economic use of composite materials which had been explored previously (refs. 3 and 4). These results are shown in table 8. The buckling strengths of the equivalent-weight aluminum-alloy and titanium-alloy cylinders have been calculated. The aluminum-alloy cylinder having a thickness of 0.038 in (0.096 cm), a length of 10 in (25.4 cm) and a diameter of 6 in (15 cm) has a predicted buckling strength of 40,200 lbf-in (4,500 N-m). The similar titanium alloy cylinder, with a thickness of 0.034 in (0.076 cm) has a predicted buckling strength of 50,100 lbf-in (5,700 N-m). The analysis predicts a considerable strength-to-weight savings for a reinforced-metal specimen over the equivalent-weight metal specimen. The actual strength-to-weight savings is somewhat less than predicted, due to the relatively low load at which the composite material debonded from the metal or endcap failure occurred, for the specimens tested. The results of the tests on specimens C11 and C12 indicate that the ultimate shear strain of the graphite material in this ply configuration is about 0.0150. At failure, the shear strains in specimen AC03 were about 0.0075. The buckling failure loads, therefore, would be expected to be somewhat higher and the strength-to-weight savings would improve. Nevertheless, the strength-to-weight ratios which were obtained are larger than those obtained with unidirectionally-reinforced-metal specimens (ref. 3).

7.6 Post-Buckling Failure Behavior

As the specimen wall is loaded in torsion near the buckling load, it begins to assume the buckled wave pattern particular to that specimen configuration. At initiation of buckling and during post-buckling loading it was observed that the failure behavior of the two composite materials was different. The specimens fabricated with boron/epoxy continued to carry load in the post-buckling regime, as indicated by curves of figure 7. Deep elastic buckles, as shown in figures 8 d, e, f and h can be twisted into the boron/epoxy specimens without permanent damage. Specimens fabricated with graphite/epoxy, however, failed catastrophically soon after the maximum torque was reached. An example of this type of failure is shown in figures 8c and g.

8. CONCLUSIONS

Based on the investigation of elastic torsional buckling in thin-walled-composite cylindrical shells reported herein, the following conclusions are drawn:

1. An available computer analysis has been exercised extensively and its usefulness has been established in predicting buckling torques for several laminate configurations. The effect of uncoupling the bending and extension forces for the thin laminate, which was assumed by the analysis, has been experimentally tested and the validity of the assumption verified by the resulting agreement between analysis and experiment. Correlation factors in excess of 0.80 for experiment in relation to analysis were not uncommon for these tests. There appears to be a modeling error of approximately 8 percent between the analysis and experiment.

2. Torsional buckling strengths which differ by as much as a factor of two may result from reversing the direction of twist of a thin-walled-composite cylinder. This is of potential importance in applications where reversals of loading may occur and in selection of a lay-up configuration for a single direction of torque.

3. The buckling results obtained by reversing the stacking sequence in a laminated thin-walled cylinder loaded in torsion have been shown to be equivalent to the buckling results obtained by reversing the direction of twist on the original stacking sequence.

4. Shear stress-shear strain curves computed from the results of tests on large composite, and composite-reinforced-metal torsional specimens, and the principal elastic moduli (E_{11}), and in-plane shear moduli (G_{12}) computed from these curves, have been given.

5. A 2:1 linear scaling of cylinder dimensions, while maintaining constant L/r and D/t ratios, resulted in buckling torques which differed by about an order of magnitude, while the shear stresses at failure were approximately equal.

6. An "optimum" stacking sequence which produced significant increases in the predicted and measured buckling loads for a four-ply cylinder was determined. This results in considerable increases in the strength-to-weight ratio over other sequences examined herein and in reference 3.

7. The "optimum" stacking sequence was also used for aluminum-alloy and titanium-alloy cylinders reinforced on their outer surfaces with composite materials. This sequence resulted in significant increases in the strength-to-weight ratio over several other ply sequences tested. There is a tendency for these higher strength specimens to fail by mechanisms other than elastic buckling.

8. Boron/epoxy cylinders which fail by elastic torsional buckling have considerably more post-buckling strength than similar cylinders fabricated from graphite/epoxy.

9. REFERENCES

1. Dexter, H. B., Flight Service Evaluation of Composite Structural Components, Proceedings of the Conference on Fibrous Composites in Flight Vehicle Design (Dayton, September 1972 AFFDL-TR-72-130, pp 369-407 December 1972.

2. Davis, J. G., Jr., Evaluation of Metal Structures Selectively Reinforced with Filamentary Composites for Space Shuttle Application, ibid., pp 445-489.

3. Marlowe, D. E., Torsional Instabilities in Composite and Composite-Reinforced Aluminum-Alloy Thin-Walled Cylinders, NBS Technical Note No. 728, 1972.

4. Marlowe, D. E., Sushinsky, G. F., and Dexter, H. B., Elastic

Torsional Buckling of Thin-Walled Composite Cylinders, Composite Materials: Testing and Design (Third Conference) Williamsburg, Va., March 1973 ASTM STP 546, Amercian Society for Testing and Materials, pp 84-108, 1974.

5. ASTM Designation E380-72, Standard Metric Practice Guide, American Society for Testing and Materials, Philadelphia, Pennsylvania.

6. Chao, Tung-Lai, Minimum Weight Design of Stiffened Fiber Composite Cylinders, AFML TR 69-251, September 1969.

7. Timoshenko, S. P., and Gere, J. M., Theory of Elastic Stability, McGraw Hill Book Co., Inc., New York, 1961.

8. Wu, Chi-Hwa, Buckling of Anisotropic Circular Cylindrical Shells, Doctoral Dissertation, Case-Western Reserve Univ., June 1971.

9. Davis, J. G., Tube Fabricating Process, United States Patent No. 3,607,495, September 1971.

10. Chwirut, D. J., Coordinator, Research and Testing Facilities of the Engineering Mechanics Section, National Bureau of Standards, Washington, D. C., NBS Special Publication No. 370, January 1973.

11. Batdorf, S. B., Stein, M., and Schildcrout, M., Critical Stress of Thin Walled Cylinders in Torsion, NACA TN 1344, 1947.

Table 1 - Specimen Designations

Designation	Material	Specimen length	
		in	cm
T	titanium alloy	10.0	25.4
B	boron/epoxy	10.0	25.4
BL	boron/epoxy	20.0	50.8
BLL	boron/epoxy	40.0	101.6
C	graphite/epoxy	10.0	25.4
CL	graphite/epoxy	20.0	50.8
AC	graphite/epoxy reinforced aluminum alloy	10.0	25.4
TB	boron/epoxy-reinforced titanium alloy	10.0	25.4
TC	graphite/epoxy-reinforced titanium alloy	10.0	25.4

Table 2 - Dimensions of Torsional Specimens

Specimen No.	Specimen length		Specimen diameter		Metal thickness		Composite thickness		Nominal L/r	Nominal D/t	Ply orientation	Filament volume fraction
	in	cm	in	cm	in	cm	in	cm			degrees	percent
All-metal Specimens												
T01	10.0	25.4	5.990	15.21	0.023	0.058	---	---	3.3	300	---	---
T02	10.0	25.4	5.994	15.22	.026	.066	---	---	3.3	300	---	---
Unidirectional Composite Specimens												
B07	10.0	25.4	5.964	15.15	---	---	.022	.056	3.3	300	(0, 0)s	47.4
B08	10.0	25.4	5.970	15.16	---	---	.022	.056	3.3	300	(0, 0)s	48.2
BL07	20.0	50.8	6.016	15.28	---	---	.023	.058	6.7	300	(45, 45)s	45.0
BL05	20.0	50.8	6.000	15.24	---	---	.022	.056	6.7	300	(-45, -45)s	46.5
BL06	20.0	50.8	6.066	15.41	---	---	.021	.053	6.7	300	(-45, -45)s	48.2
C01	10.0	25.4	6.003	15.25	---	---	.025	.064	3.3	300	(0, 0)s	51.4
C05	10.0	25.4	6.016	15.28	---	---	.024	.061	3.3	300	(0, 0)s	52.2
Effect of Stacking Sequence												
B01	10.0	25.4	6.008	15.26	---	---	0.022	0.056	3.3	300	(-45, +45)s	47.4
B02	10.0	25.4	6.008	15.26	---	---	.022	.056	3.3	300	(-45, +45)s	47.4
B03	10.0	25.4	6.012	15.27	---	---	.022	.056	3.3	300	(+45, -45)s	46.5
B04	10.0	25.4	6.000	15.24	---	---	.022	.056	3.3	300	(+45, -45)s	46.5
C04	10.0	25.4	6.001	15.24	---	---	.023	.058	3.3	300	(+45, -45)s	53.9
C08	10.0	25.4	5.988	15.21	---	---	.024	.061	3.3	300	(+45, -45)s	48.8
C06	10.0	25.4	6.016	15.28	---	---	.024	.061	3.3	300	(-45, +45)s	53.9
C07	10.0	25.4	6.002	15.25	---	---	.024	.061	3.3	300	(-45, +45)s	52.2
Effect of Linear Scaling												
BLL01	40.0	101.6	6.056	15.38	---	---	0.023	0.058	13.3	300	(-45, +45)s	45.0
BLL02	40.0	101.6	6.039	15.34	---	---	.024	.061	13.3	300	(-45, +45)s	44.3

continued

Table 2 - Dimensions of Torsional Specimens

Specimen No.	Specimen length		Specimen diameter		Metal thickness		Composite thickness		Nominal L/r	Nominal D/t	Ply orientation	Filament volume fraction
	in	cm	in	cm	in	cm	in	cm			degrees	percent
Effect of Linear Scaling - continued												
BL10	20.0	50.8	5.992	15.22	---	---	0.023	0.058	6.7	300	(-45, +45)s	45.0
BL11	20.0	50.8	6.074	15.43	---	---	.023	.058	6.7	300	(-45, +45)s	46.5
B05	10.0	25.4	3.030	7.696	---	---	.022	.056	6.7	150	(+45, -45)s	46.5
B06	10.0	25.4	3.028	7.691	---	---	.022	.056	6.7	150	(+45, -45)s	46.5
BL08	20.0	50.8	6.048	15.36	---	---	.046	.117	6.7	150	(-45, -45, +45, +45)s	45.7
BL09	20.0	50.8	6.036	15.33	---	---	.044	.112	6.7	150	(-45, -45, -45, +45)s(b)	47.4
C09	10.0	25.4	3.036	7.711	---	---	.025	.064	6.7	150	(-45, +45)s	50.5
C10	10.0	25.4	2.992	7.600	---	---	.024	.061	6.7	150	(-45, +45)s	53.0
CL01	20.0	50.8	6.108	15.51	---	---	.049	.125	6.7	150	(-45, -45, +45, +45)s	50.5
CL02	20.0	50.8	6.093	15.48	---	---	.048	.122	6.7	150	(-45, -45, +45, +45)s	50.5
Optimum Angle Specimens												
B09	10.0	25.4	6.013	15.27	---	---	0.023	0.058	3.3	300	(-82.5, 20, 30, -82.5)(c)	45.0
B10	10.0	25.4	5.959	15.14	---	---	.023	.058	3.3	300	(-82.5, 30, 20, -82.5)	46.5
C11	10.0	25.4	5.996	15.23	---	---	.024	.061	3.3	300	(-82.5, 30, 20, -82.5)	48.8
C12	10.0	25.4	5.976	15.18	---	---	.024	.061	3.3	300	(-82.5, 30, 20, -82.5)	50.5
Composite - Reinforced Metal Specimens												
AC02	10.0	25.4	5.967	15.16	0.023	0.058	0.032(a)	0.081	3.3	120	(-82.5, 30, 20, -82.5)	
AC03	10.0	25.4	5.964	15.15	.022	.056	.032(a)	.081	3.3	120	(-82.5, 30, 20, -82.5)	

continued

Table 2 - Dimensions of Torsional Specimens

Specimen No.	Specimen length		Specimen diameter		Metal thickness		Composite thickness		Nominal L/r	Nominal D/t	Ply orientation	Filament volume fraction
	in	cm	in	cm	in	cm	in	cm			degrees	percent
Composite - Reinforced Metal Specimens - continued												
TB01	10.0	25.4	5.995	15.23	0.027	0.068	0.028(a)	0.071	3.3	120	(-82.5, 30, 20, -82.5)	
TB02	10.0	25.4	5.996	15.23	.025	.064	.029(a)	.074	3.3	120	(-82.5, 30, 20, -82.5)	
TC02	10.0	25.4	6.002	15.24	.024	.061	.032(a)	.081	3.3	120	(-82.5, 30, 20, -82.5)	
TC03	10.0	25.4	6.001	15.24	.025	.064	.031(a)	.079	3.3	120	(-82.5, 30, 20, -82.5)	

(a) Includes 0.005-in (0.013-cm) thickness of film-epoxy adhesive.

(b) The analysis indicated that this specimen stacking sequence was equally as strong as the balanced configuration of Specimen BL08.

(c) This stacking sequence is the result of a fabrication error.

Table 3 - Average Material Properties

Material	Elastic modulus in the direction of				In-plane shear modulus		Principal in-plane Poisson's ratio
	Major axis		Minor axis				
	lbf/in^2	N/m^2	lbf/in^2	N/m^2	lbf/in^2	N/m^2	
Aluminum alloy	10.2×10^6	70×10^9	10.2×10^6	70×10^9	3.9×10^6	27×10^9	0.33
Titanium alloy	16.0	110	16.0	110	6.3	43	.33
Boron/epoxy	31.0	219	2.5	17	0.59	4.1	.21
Graphite/epoxy	30.9	213	1.1	7.6	0.53	3.7	.28

Table 4 - Elastic Properties of Torsional Specimens

Tube No.	Ply Orientation	Effective Elastic Modulus E_{11} theor.		E_{11} exp.		Effective Shear Modulus G_{12} theor.		G_{12} exp.	
	degrees	lbf/in^2	N/m^2	lbf/in^2	N/m^2	lbf/in^2	N/m^2	lbf/in^2	N/m^2
All Metal Specimens									
T01	--	16.0×10^6	11.0×10^{10}	16.5×10^6	11.4×10^{10}	6.2×10^6	4.3×10^{10}	6.3×10^6	4.3×10^{10}
T02	--	16.0	11.0	17.6	12.1	6.2	4.3	6.3	4.3
Unidirectional Composite Specimens									
B07	$(0,0)_s$	27.4	18.9	28.0	19.3	0.58	0.40	0.65	0.45
B08	$(0,0)_s$	27.4	18.9	28.0	19.3	0.58	0.40	0.66	0.46
BL07	$(+45, +45)_s$	1.8	1.2	1.8	1.2	1.9	1.3	1.7	1.1
BL05	$(-45, -45)_s$	1.8	1.2	1.5	1.0	1.9	1.3	1.6	1.1
BL06	$(-45, -45)_s$	1.8	1.2	1.7	1.1	2.0	1.4	1.6	1.1
C01	$(0,0)s$	25.4	17.5	19.5	13.4	0.53	0.36	0.51	0.35
C05	$(0,0)s$	26.6	18.3	22.3	15.4	0.53	0.36	0.55	0.38
Effect of Stacking Sequence									
B01	$(-45, +45)_s$	2.2	1.5	2.4	1.6	7.2	5.0	7.2	5.0
B02	$(-45, +45)_s$	2.2	1.5	2.4	1.6	7.2	5.0	6.8	4.7
B03	$(+45, -45)_s$	2.2	1.5	2.0	1.4	7.1	4.9	6.1	4.2
B04	$(+45, -45)_s$	2.2	1.5	2.0	1.4	7.1	4.9	6.4	4.4
C04	$(+45, -45)_s$	2.0	1.4	2.0	1.4	7.1	4.9	5.4	3.7
C08	$(+45, -45)_s$	2.0	1.4	1.8	1.2	6.8	4.7	5.7	3.9
C06	$(-45, +45)_s$	2.0	1.4	1.9	1.3	6.9	4.8	5.6	3.9
C07	$(-45, +45)_s$	2.0	1.4	1.8	1.2	6.8	4.7	5.9	4.1

Continued

Table 4 - Elastic Properties of Torsional Specimens

Tube No.	Ply Orientation	Effective Elastic Modulus E_{11} theor.		E_{11} exp.		Effective Shear Modulus G_{12} theor.		G_{12} exp.	
	degrees	lbf/in^2	N/m^2	lbf/in^2	N/m^2	lbf/in^2	N/m^2	lbf/in^2	N/m^2
Effect of Linear Scaling									
BLL01	$(-45, +45)_s$	2.1×10^6	1.4×10^6	--	--	6.8×10^6	4.7×10^{10}	6.0×10^6	4.1×10^{10}
BLL02	$(-45, +45)_s$	2.1	1.4	--	--	6.7	4.6	6.7	4.6
BL10	$(-45, +45)_s$	2.1	1.4	2.2×10^6	1.5×10^6	6.8	4.7	6.4	4.4
BL11	$(-45, +45)_s$	2.2	1.5	2.1	1.4	7.1	4.9	6.4	4.4
B05	$(+45, -45)_s$	2.2	1.5	1.9	1.2	7.1	4.9	6.9	4.8
B06	$(+45, -45)_s$	2.2	1.5	2.1	1.4	7.1	4.9	7.1	4.9
BL08	$(-45, -45, +45, +45)_s$	2.2	1.5	2.2	1.5	7.0	4.8	6.9	4.8
BL09	$(-45, -45, -45, +45)_s$	2.1	1.4	2.1	1.4	5.9	4.1	5.6	3.9
C09	$(-45, +45)_s$	2.0	1.4	1.7	1.2	6.6	4.6	5.7	3.9
C10	$(-45, +45)_s$	2.0	1.4	1.9	1.3	6.8	4.7	6.1	4.2
CL01	$(-45, -45, +45, +45)_s$	2.0	1.4	1.9	1.3	6.7	4.6	6.7	4.6
CL02	$(-45, -45, +45, +45)_s$	2.0	1.4	--	--	6.8	4.7	5.6	3.9
Optimum Angle Specimens									
B09	(-82.5, 20, 30, -82.5)	3.9	2.7	3.6	2.5	1.0	0.69	0.91	0.63
B10	(-82.5, 30, 20, -82.5)	4.0	2.8	3.9	2.7	1.0	0.69	1.1	0.76
C11	(-82.5, 30, 20, -82.5)	3.5	2.4	3.2	2.2	0.87	0.60	0.97	0.67
C12	(-82.5, 30, 20, -82.5)	3.2	2.2	3.2	2.2	0.87	0.60	0.88	0.61

Continued

Table 4 - Elastic Properties of Torsional Specimens

Tube No.	Ply Orientation	Effective Elastic Modulus E_{11} theor.		E_{11} exp.		Effective Shear Modulus G_{12} theor.		G_{12} exp.	
	degrees	lbf/in^2	N/m^2	lbf/in^2	N/m^2	lbf/in^2	N/m^2	lbf/in^2	N/m^2
Composite - Reinforced Metal Specimens									
AC02	(-82.5, 30, 20, -82.5)	7.5×10^6	5.2×10^6	6.5×10^6	4.5×10^{10}	2.4×10^6	1.6×10^{10}	2.3×10^6	1.6×10^{10}
AC03	(-82.5, 30, 20, -82.5)	7.5	5.2	7.2	5.0	2.4	1.6	2.2	1.5
TB01	(-82.5, 30, 20, -82.5)	11.3	7.8	12.4	8.5	4.0	2.8	3.6	2.5
TB02	(-82.5, 30, 20, -82.5)	11.0	7.6	12.0	8.3	3.8	2.6	3.6	2.5
TC02	(-82.5, 30, 20, -82.5)	10.4	7.2	9.8	6.8	3.6	2.5	3.2	2.2
TC03	(-82.5, 30, 20, -82.5)	--	--	--	--	3.7	2.6	3.4	2.3

Table 5 - Buckling Torques of Torsional Specimens

Specimen No.	Ply orientation	Nominal L/r	Nominal D/t	Loading direction	Predicted buckling torque		Maximum measured torque		Correlation factor
	degrees				lbf-in	N-m	lbf-in	N-m	
All-metal Specimens									
T01	---	3.3	300	Neg	21100	2380	21900	2470	1.04
T02	---	3.3	300	Neg	27000	3050	29500	3330	1.09
Unidirectional Composite Specimens									
B07	$(0, 0)_s$	3.3	300	Neg	3300	373	3010	340	0.91
B08	$(0, 0)_s$	3.3	300	Neg	3220	364	3050	345	.95
BL07	$(45, 45)_s$	6.7	300	Neg	3260	368	2830	320	.87
BL05	$(-45, -45)_s$	6.7	300	Neg	5430	614	3290(a)	372(a)	.61(a)
BL06	$(-45, -45)_s$	6.7	300	Neg	5060	572	3950(a)	446(a)	.78(a)
C01	$(0, 0)_s$	3.3	300	Neg	3010	340	2170	245	.72
C05	$(0, 0)_s$	3.3	300	Neg	2720	307	2040	230	.75
Effect of Stacking Sequence									
B01	$(-45, +45)_s$	3.3	300	Neg	10300	1160	9220	1040	.90
				Pos	5360	606	4750	537	.89
B02	$(-45, +45)_s$	3.3	300	Neg	10300	1160	9300	1050	.90
				Pos	5360	606	4600	520	.86
B03	$(+45, -45)_s$	3.3	300	Neg	5600	633	4590	519	.82
				Pos	10800	1220	9250	1040	.86
B04	$(+45, -45)_s$	3.3	300	Neg	5580	631	4380	495	.78
				Pos	10800	1220	9430	1060	.87
C04	$(+45, -45)_s$	3.3	300	Neg	5000	565	4500	508	.90
				Pos	10600	1198	9100	1030	.86
C08	$(+45, -45)_s$	3.3	300	Neg	5640	637	4800	542	.85
				Pos	12000	1360	9880	1120	.82
C06	$(-45, +45)_s$	3.3	300	Neg	11500	1299	8380	947	.73
				Pos	5430	613	3980	450	.73
C07	$(-45, +45)_s$	3.3	300	Neg	12000	1356	8990	1020	.75
				Pos	5640	637	4320	488	.77

continued

Table 5 - Buckling Torques of Torsional Specimens

Specimen No.	Ply orientation degrees	Nominal L/r	Nominal D/t	Loading direction	Predicted buckling torque lbf-in	Predicted buckling torque N-m	Maximum measured torque lbf-in	Maximum measured torque N-m	Correlation factor
Effect of Linear Scaling									
BLL01	(-45, +45)s	13.33	300	Neg	4080	461	3570	403	0.88
				Pos	2670	302	2400	271	.90
BLL02	(-45, +45)s	13.33	300	Neg	4170	471	3460	391	.83
				Pos	2740	310	2430	274	.89
BL10	(-45, +45)s	6.7	300	Neg	6880	777	6110	690	.89
				Pos	3950	446	3450	390	.87
BL11	(-45, +45)s	6.7	300	Neg	6530	738	6030	681	.92
				Pos	3740	423	3500	396	.94
B05	(+45, -45)s	6.7	150	Neg	2270	256	1750	198	.77
				Pos	4180	472	3500	396	.84
B06	(+45, -45)s	6.7	150	Neg	2270	256	1960	221	.86
BL08	(-45, -45, +45, +45)s	6.7	150	Neg	34900	3940	30550	3450	.88
				Pos	18900	2140	16700	1890	.88
BL09	(-45, -45, -45, +45)s	6.7	150	Neg	33100	3740	30700	3470	.93
				Pos	14200	1600	13450	1520	.95
C09	(-45, +45)s	6.7	150	Neg	5120	578	3540	400	.69
				Pos	2500	282	1970	223	.79
C10	(-45, +45)s	6.7	150	Neg	4700	531	3560	402	.76
				Pos	2300	260	1870	211	.84
CL01	(-45, -45, +45, +45)s	6.7	150	Neg	39500	4460	24500(b)	2770(b)	.62(b)
CL02	(-45, -45, +45, +45)s	6.7	150	Neg	37800	4270	22300(b)	2520(b)	.59(b)
Optimum Angle Specimens									
B09	(-82.5, 20, 30, -82.5)	3.3	300	Neg	21500	2429	17000	1921	.79
B10	(-82.5, 30, 20, -82.5)	3.3	300	Neg	20400	2305	18000	2034	.88
				Pos	7260	820	5400	610	.74
C11	(-82.5, 30, 20, -82.5)	3.3	300	Neg	22200	2508	13600	1536	.61
C12	(-82.5, 30, 20, -82.5)	3.3	300	Neg	23100	2610	12450	1407	.54

continued

Table 5 - Buckling Torques of Torsional Specimens

Specimen No.	Ply orientation	Nominal L/r	Nominal D/t	Loading direction	Predicted buckling torque		Maximum measured torque		Correlation factor
	degrees				lbf-in	N-m	lbf-in	N-m	
Composite - Reinforced Metal Specimens									
AC02	(-82.5, 30, 20, -82.5)	3.3	120	Neg	85800	9694	31250(c)	3531(c)	0.36(c)
AC03	(-82.5, 30, 20, -82.5)	3.3	120	Neg	85700	9683	43000(c)	4745(c)	.49(c)
TB01	(-82.5, 30, 20, -82.5)	3.3	120	Neg	118000	13332	86100	9728	.73
TB02	(-82.5, 30, 20, -82.5)	3.3	120	Neg	111000	12541	93500(c)	10564(c)	.84(c)
TC02	(-82.5, 30, 20, -82.5)	3.3	120	Neg	112000	12654	63100	7129	.56
TC03	(-82.5, 30, 20, -82.5)	3.3	120	Neg	115000	12993	75600(c)	8542(c)	.66(c)

(a) Matrix tension failure.

(b) Catastrophic failure without evidence of prior buckling.

(c) End cap failure; buckling did not occur.

Table 6 - Effects of Stacking Sequence and Loading Direction

Tube No.	Ply orientation	Loading direction	Predicted buckling torque		Experimental: Maximum measured torque		Experimental: Shear stress	
	degrees		lbf-in	N-m	lbf-in	N-m	lbf/in^2	N/m^2
B05	(+45, -45)s	Neg	2270	256	1750	198	5470	37.7×10^6
		Pos	4180	472	3500	395	10950	75.5
B06	(+45, -45)s	Neg	2270	256	1960	221	6100	42.1
BL08	(-45, -45, +45, +45)s	Neg	34930	3946	30550	3452	11660	80.4
		Pos	18930	2139	16700	1887	6380	44.0
BL09	(-45, -45, -45, +45)s	Neg	33130	3743	30700	3468	12140	83.7
		Pos	14240	1609	13450	1520	5320	36.7
C09	(-45, +45)s	Neg	5120	578	3540	151	9940	68.5
		Pos	2500	282	1970	223	5530	38.1
C10	(-45, +45)s	Neg	4700	531	3560	402	10320	71.2
		Pos	2300	260	1870	211	5420	37.4
CL01	(-45, -45, +45, +45)s	Neg	39520	4465	24500	2768	8540	58.9
CL02	(-45, -45, +45, +45)s	Neg	37780	4268	22300	2519	7960	54.9

Table 7 - Buckling Strengths of Optimum Ply Angle Specimens

Tube No.	Ply orientation	Loading direction	Predicted buckling torque		Experimental: Maximum measured torque		Experimental: Shear stress	
	degrees		lbf-in	N-m	lbf-in	N-m	lbf/in^2	N/m^2
B09	(-82.5, 20, 30, -82.5)	Neg	21500	2429	17000	1921	13000	89.6×10^6
B10	(-82.5, 30, 20, -82.5)	Neg	20400	2305	18000	2034	14300	98.6
		Pos	7260	820	5400	610	4280	29.5
C11	(-82.5, 30, 20, -82.5)	Neg	22200	2508	13600	1536	10400	71.7
C12	(-82.5, 30, 20, -82.5)	Neg	23100	2610	12450	1407	9170	63.2

Table 8 - Buckling Strengths of Composite-Reinforced Metal Specimens

Tube No.	Ply orientation	Loading direction	Predicted buckling torque		Experimental: Maximum measured torque		Experimental: Shear stress	
	degrees		lbf-in	N-m	lbf-in	N-m	lbf/in^2	N/m^2
AC02	(-82.5, 30, 20, -82.5)	Neg	85800	9694	31250(a)	3531(a)	10200	70.3×10^6
AC03	(-82.5, 30, 20, -82.5)	Neg	85700	9683	42000(a)	4745(a)	14200	97.9
TB01	(-82.5, 30, 20, -82,5)	Neg	118000	13332	86100	9728	27700	191.0
TB02	(-82.5, 30, 20, -82.5)	Neg	111000	12541	93500(a)	10564(a)	30700	211.7
TC02	(-82.5, 30, 20, -82.5)	Neg	112000	12651	63100	7129	20300	140.0
TC03	(-82.5, 30, 20, -82.5)	Neg	115000	12993	75600(a)	8542(a)	23900	164.8

(a) End Cap Failure; buckling did not occur

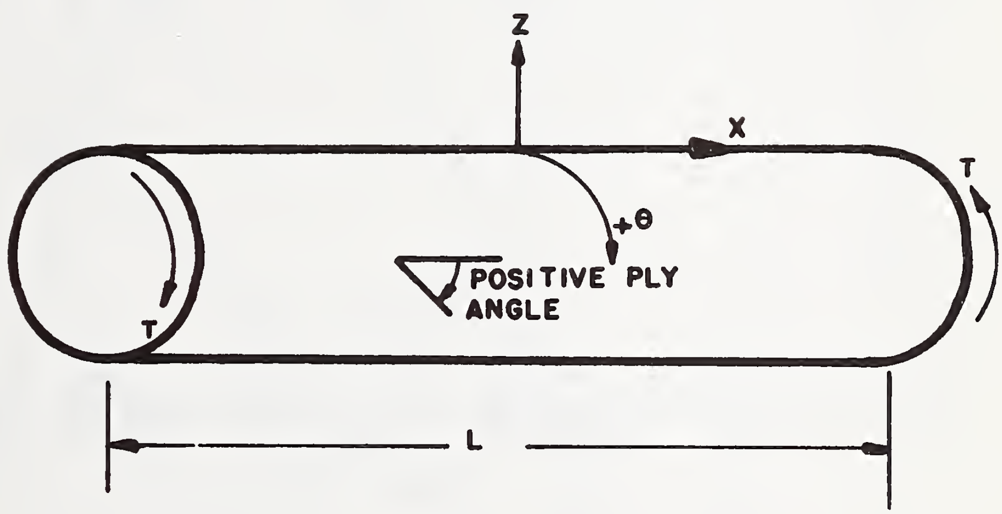

FIG. I- SHELL COORDINATE SYSTEM

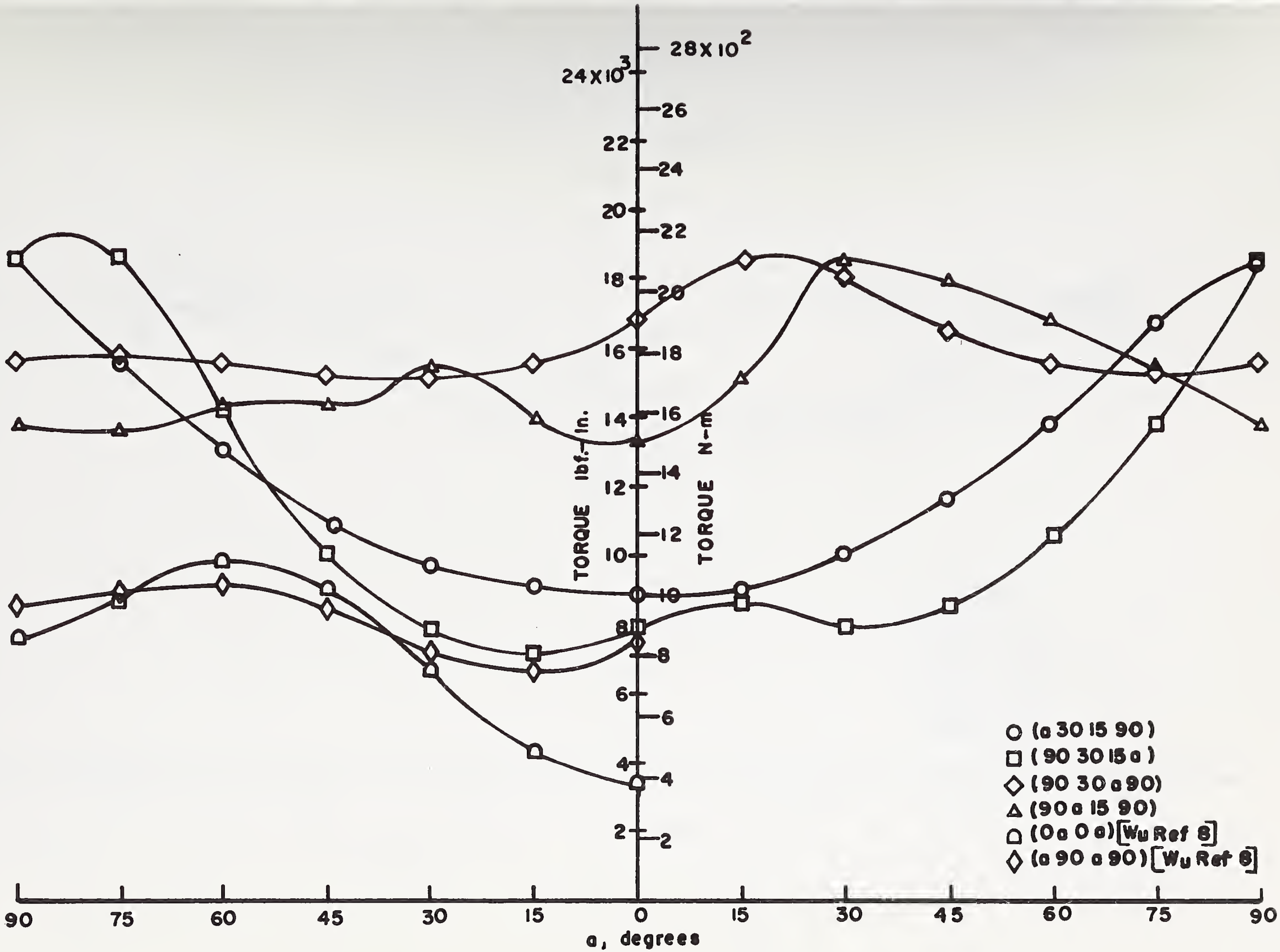

FIG. 2— EFFECT OF STACKING SEQUENCE ON BUCKLING STRENGTH OF BORON/EPOXY COMPOSITE SPECIMENS

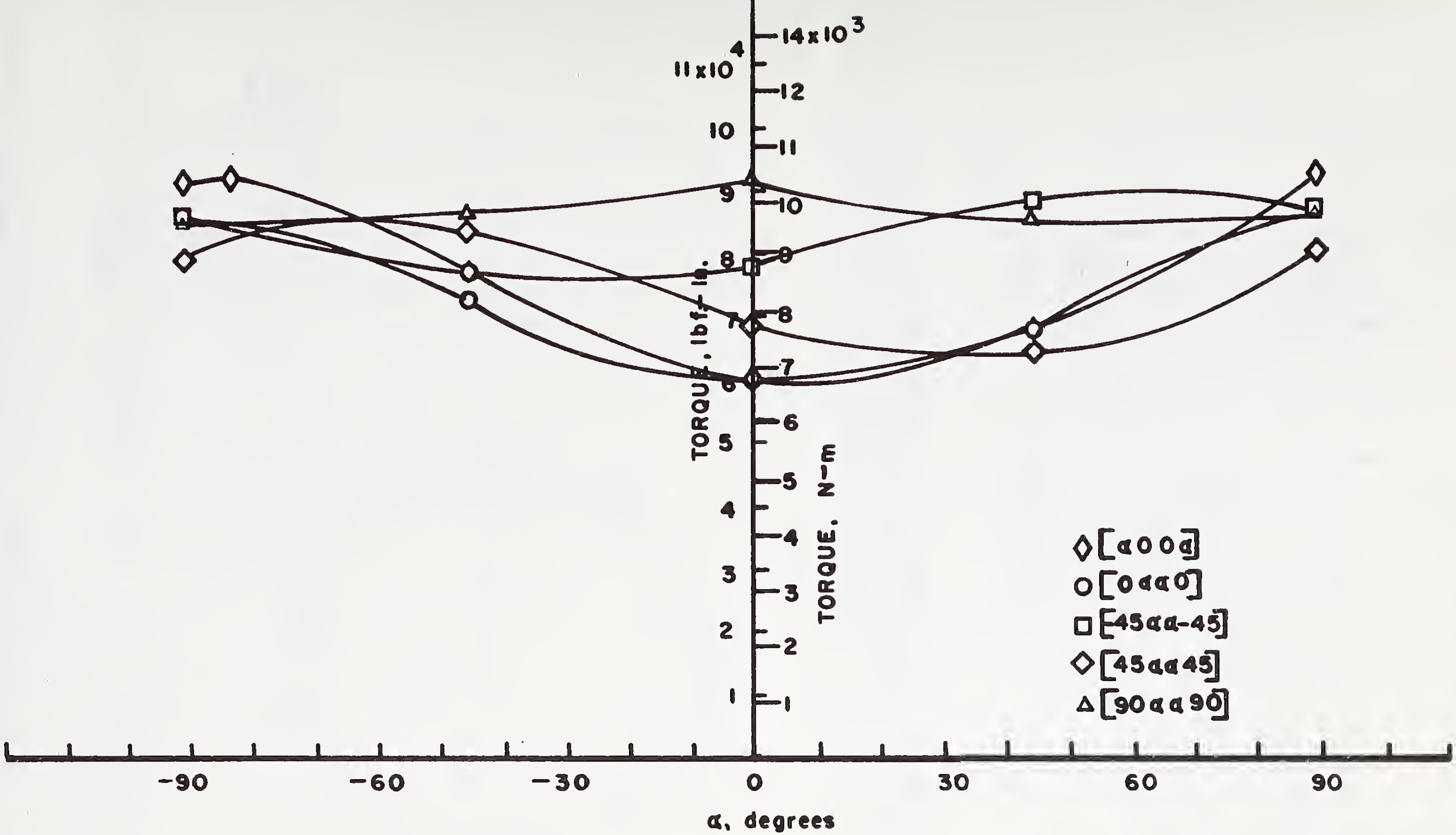

FIG. 3– EFFECT OF PLY-ANGLE CONFIGURATION ON BUCKLING STRENGTH OF BORON/EPOXY-REINFORCED TITANIUM SPECIMENS

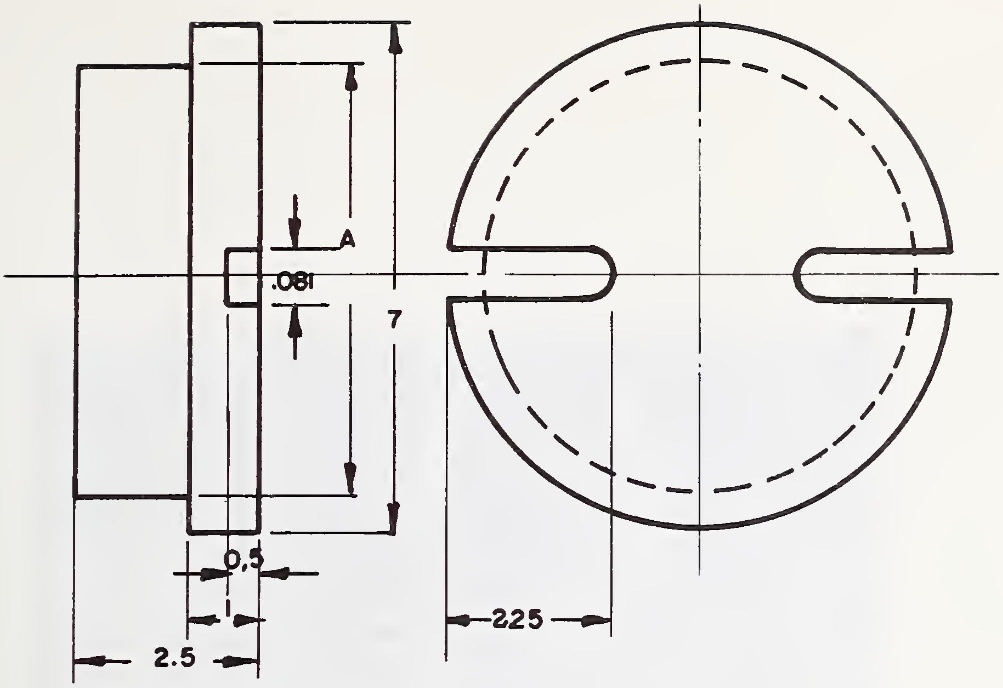

FIG. 4a END FIXTURES FOR ALL-COMPOSITE TORSION SPECIMENS. ALL DIMENSIONS ARE GIVEN IN INCHES (1 IN. = 2.54 CM)

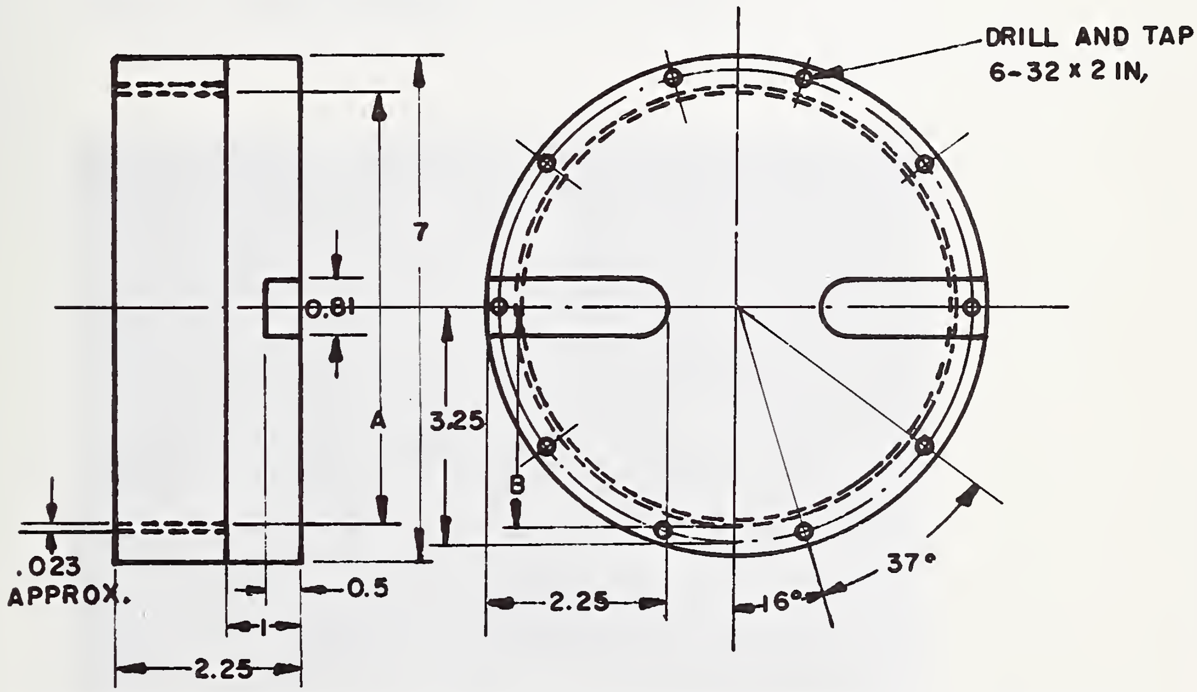

NOTES: A NOMINAL 6.00 IN.
B NOMINAL 3.02 IN.
THESE NOMINAL DIAMETERS WILL VARY WITH THE SAMPLE TESTED

FIG. 4b END FIXTURES FOR COMPOSITE-REINFORCED METAL TORSION SPECIMENS. ALL DEMENSIONS ARE GIVEN IN INCHES (1 IN. = 2.54 CM.)

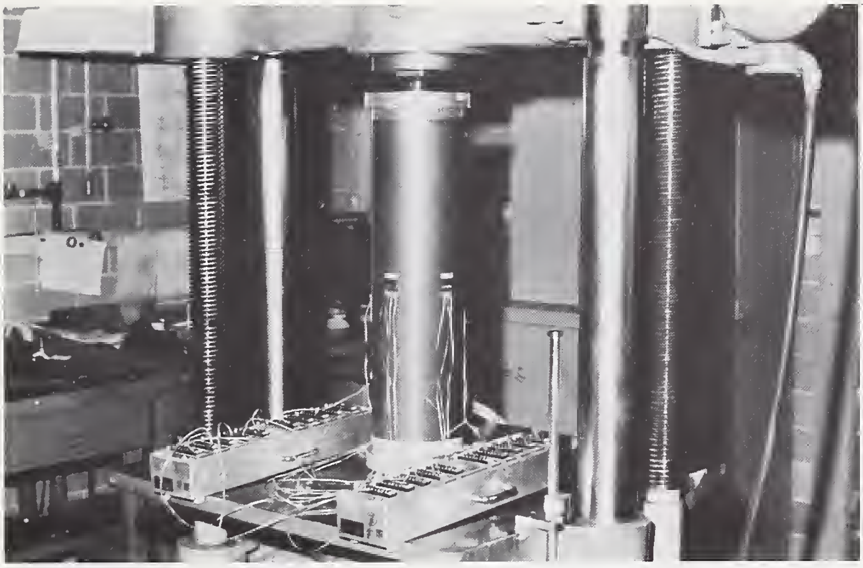

FIG. 5 COMPRESSION TEST SET-UP

FIG. 6a 40,000 lbf-in TORSION TEST SET-UP

FIG. 6b 60,000 lbf-in TORSION TEST SET-UP

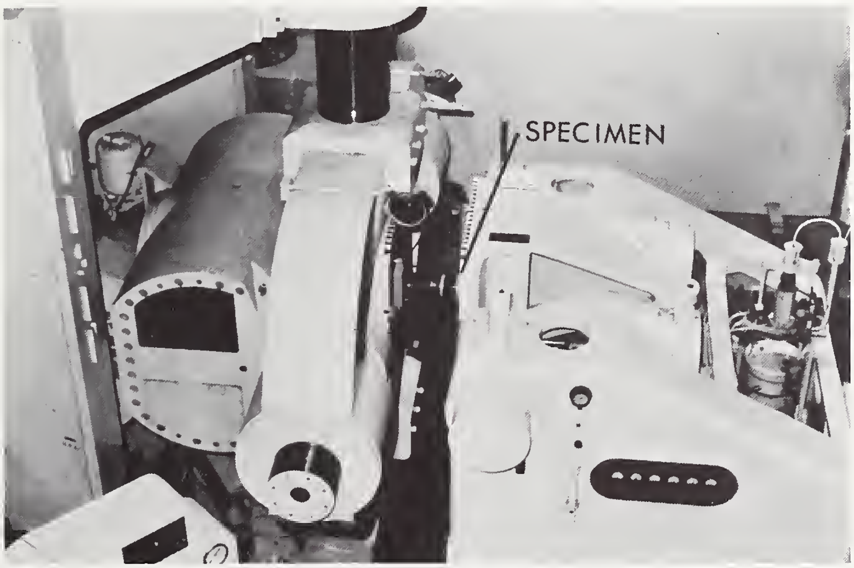

FIG. 6c 100,000 lbf-in TORSION TEST SET-UP

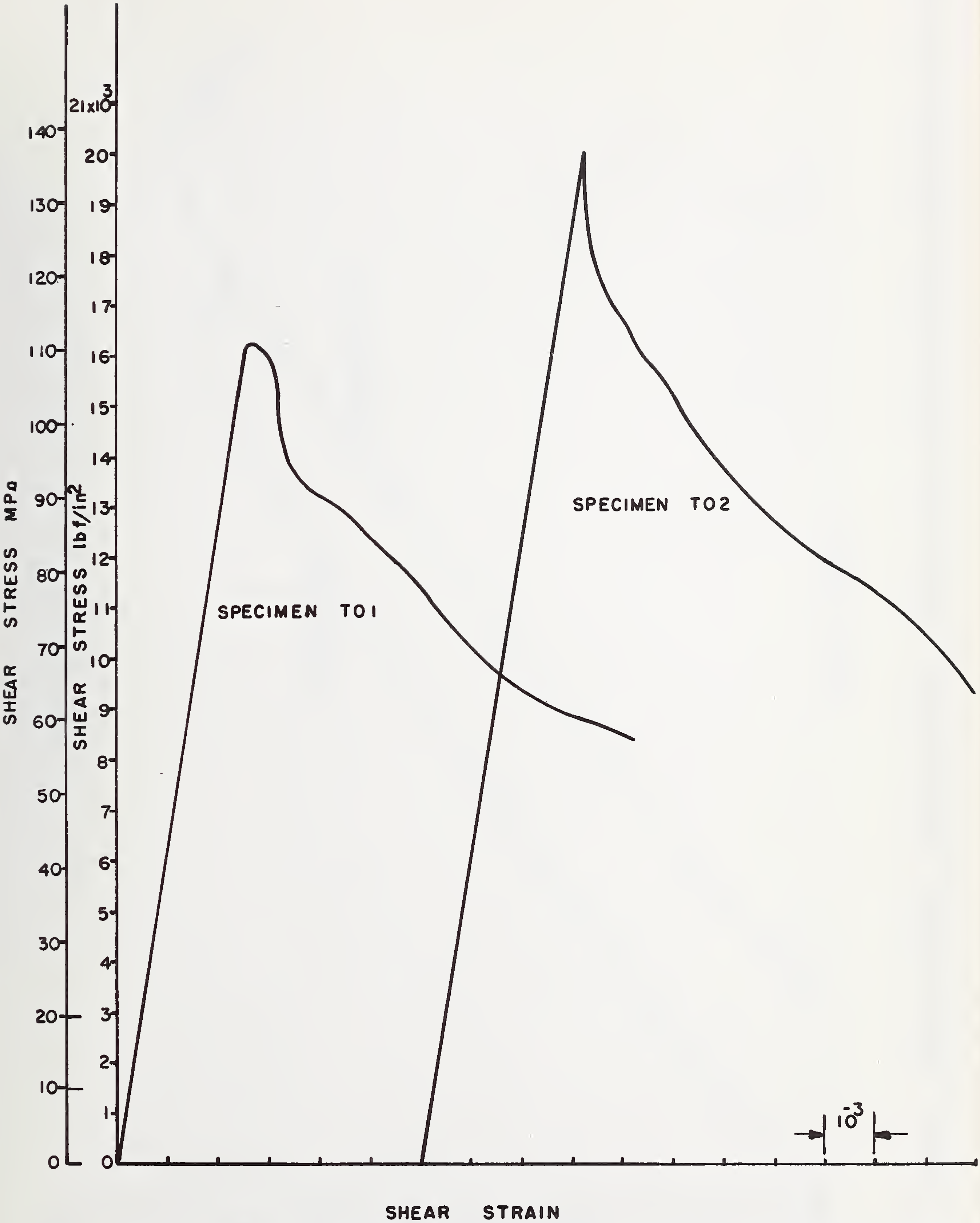

FIG. 7a — SHEAR STRESS — SHEAR STRAIN CURVES FOR ALL METAL TORSION SPECIMENS

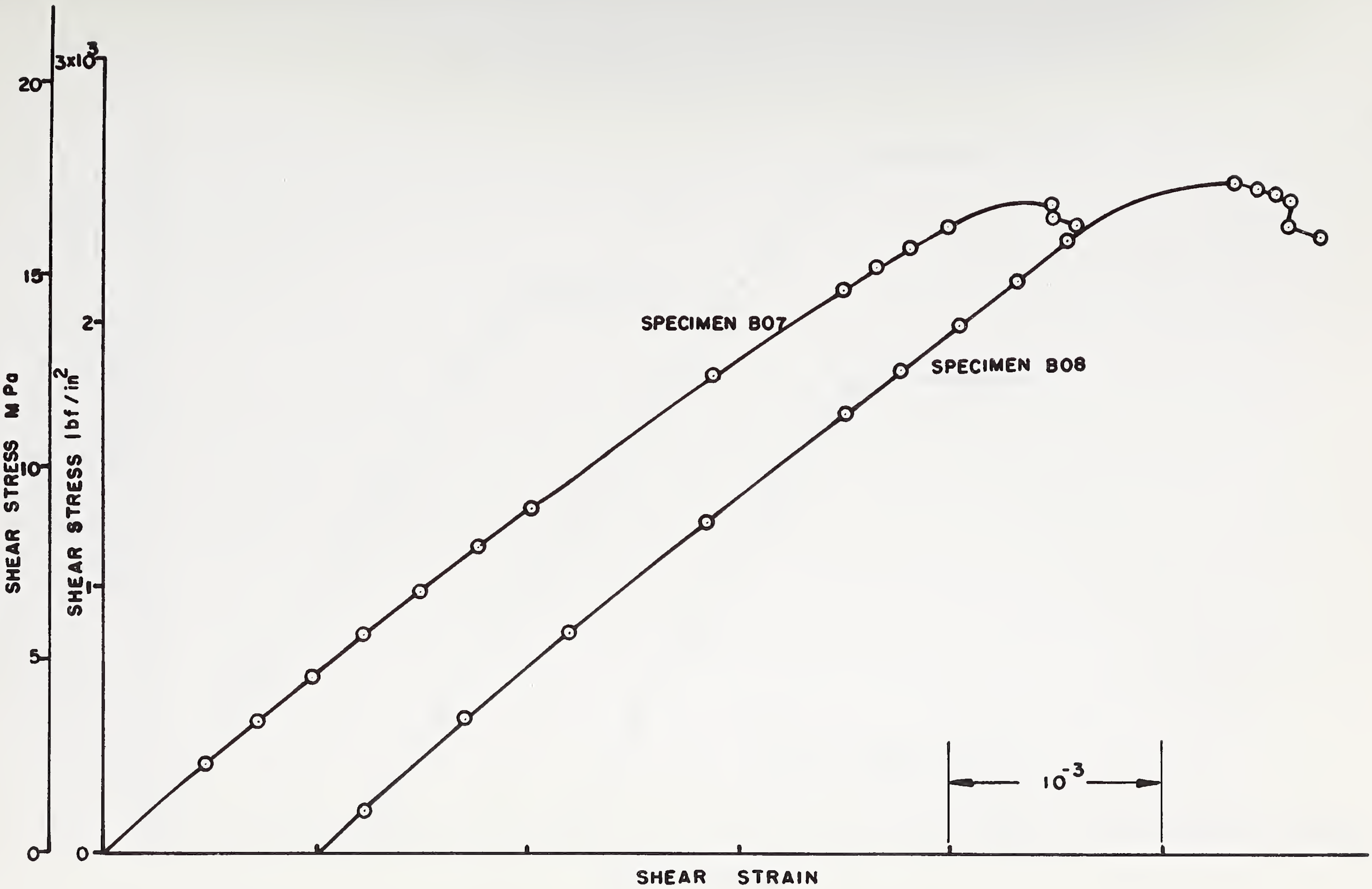

FIG. 7b— SHEAR STRESS— SHEAR STRAIN CURVES FOR UNIDIRECTIONAL COMPOSITE SPECIMENS

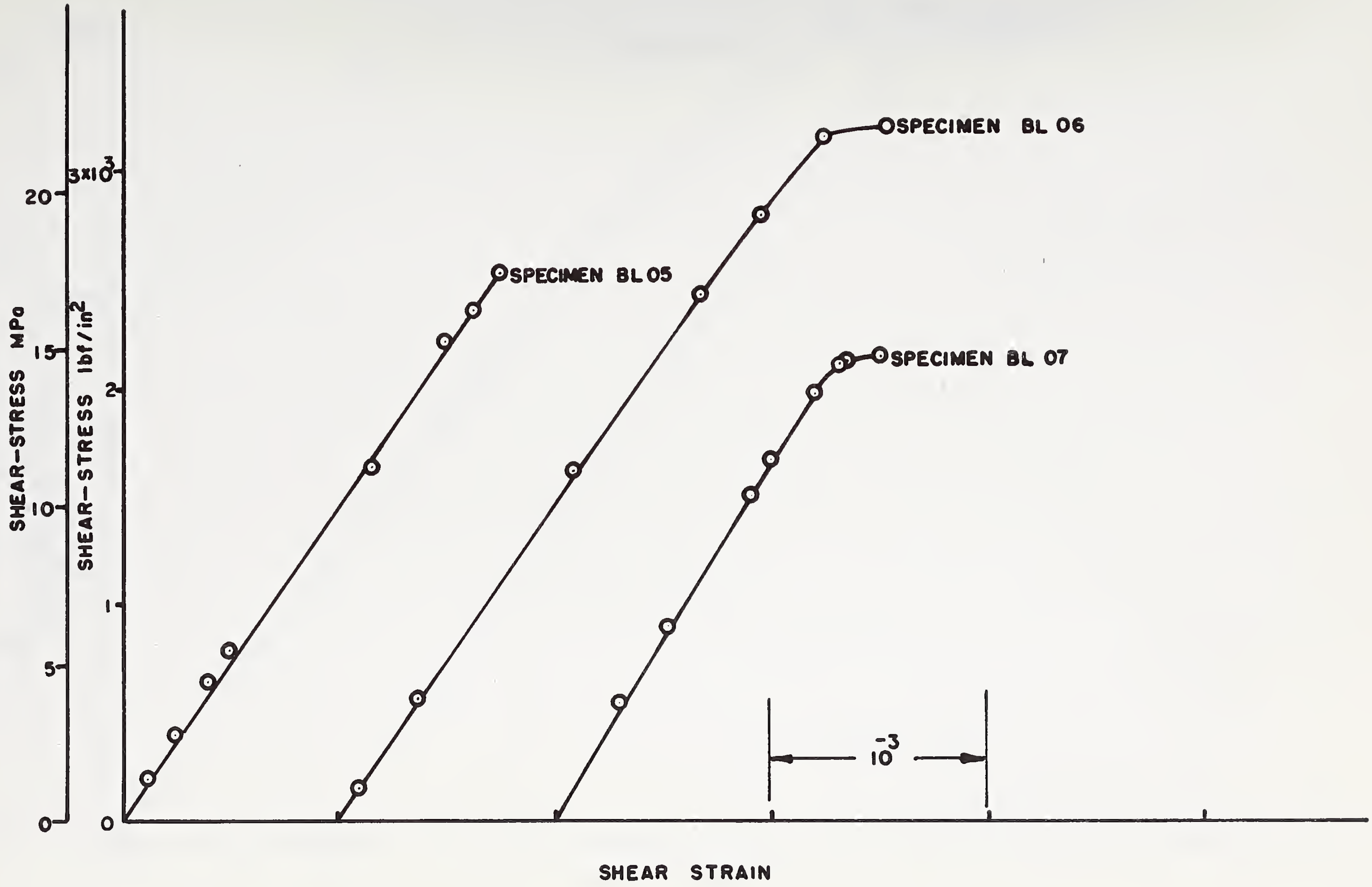

FIG. 7c—SHEAR STRESS–SHEAR STRAIN CURVES FOR UNIDIRECTIONAL COMPOSITE SPECIMENS

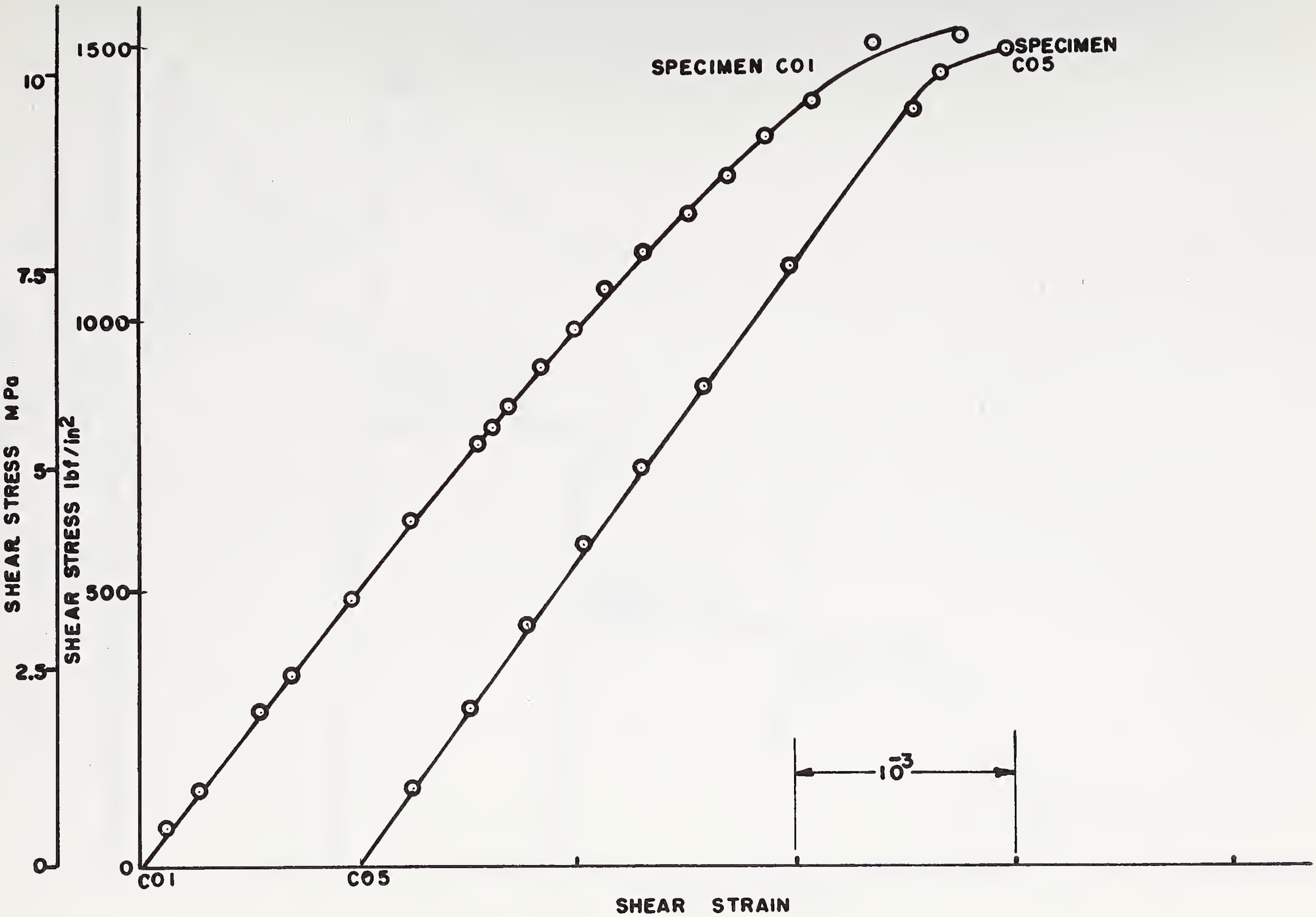

FIG. 7d–SHEAR STRESS– SHEAR STRAIN CURVES FOR UNIDIRECTIONAL COMPOSITE SPECIMENS

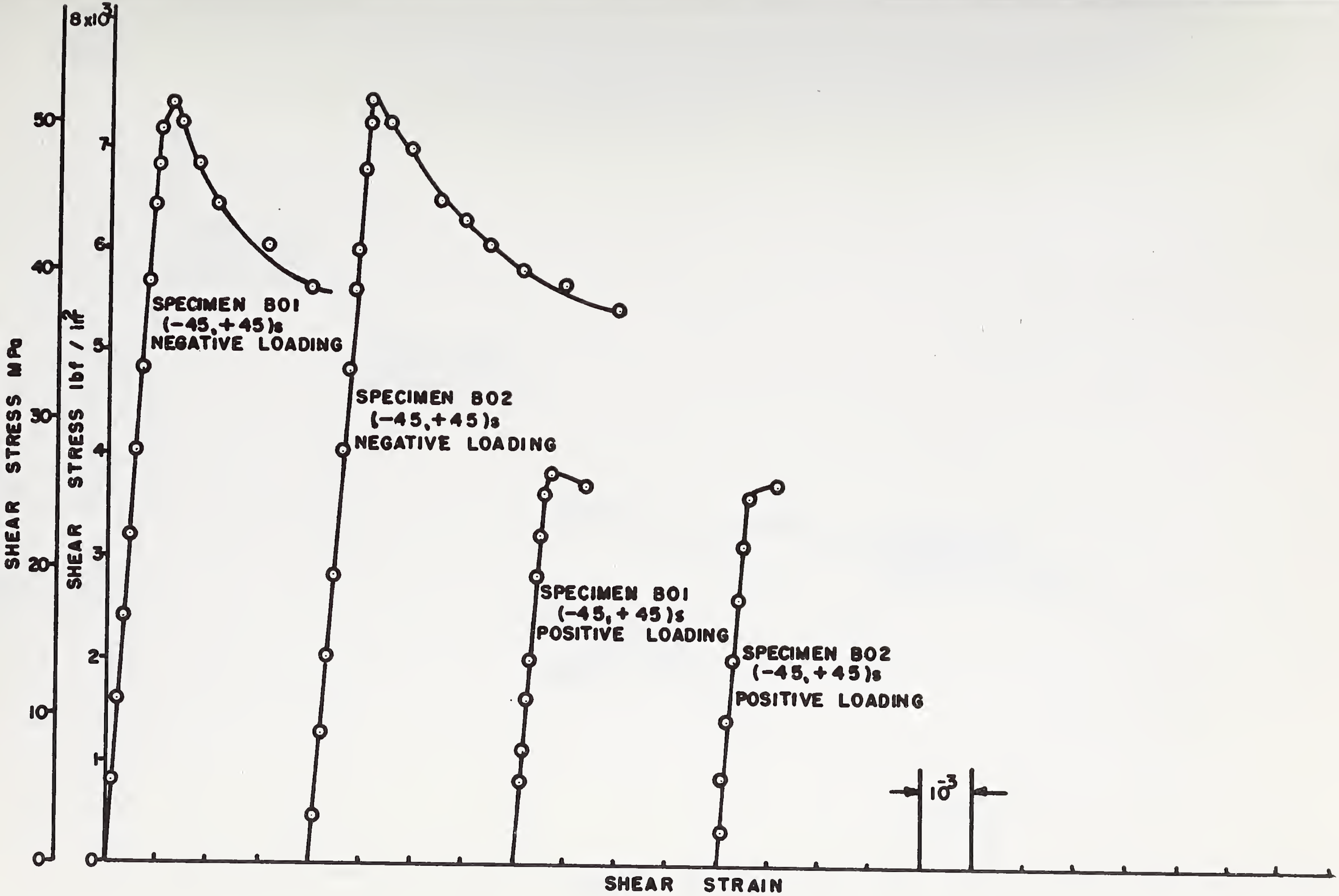

FIG. 7e– SHEAR STRESS — SHEAR STRAIN CURVES FOR SPECIMENS SHOWING EFFECTS OF STACKING SEQUENCE

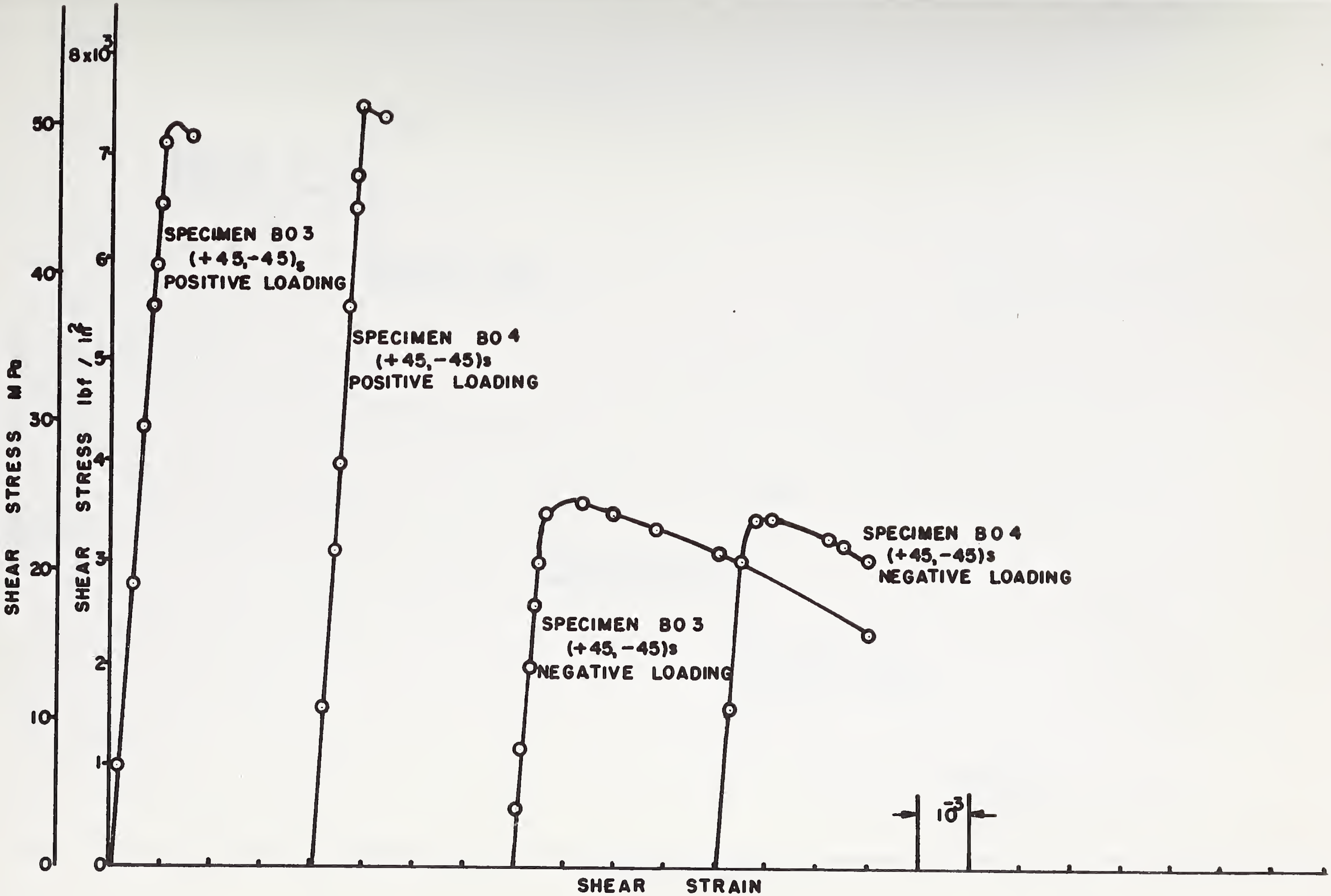

FIG. 7f– SHEAR STRESS–SHEAR STRAIN CURVES FOR SPECIMENS SHOWING EFFECTS OF STACKING SEQUENCE

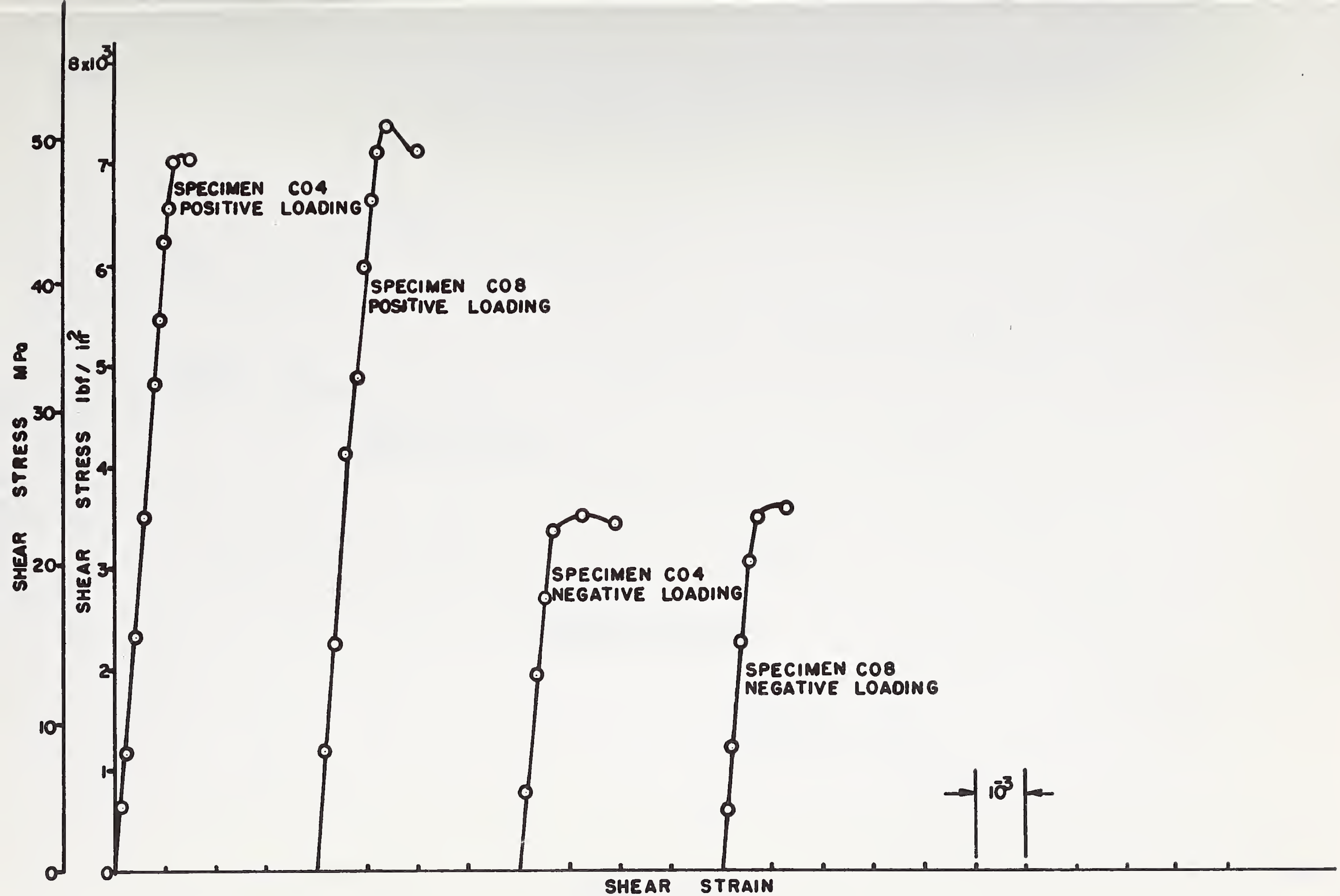

FIG. 7g — SHEAR STRESS — SHEAR STRAIN CURVES FOR SPECIMENS SHOWING EFFECTS OF STACKING SEQUENCE

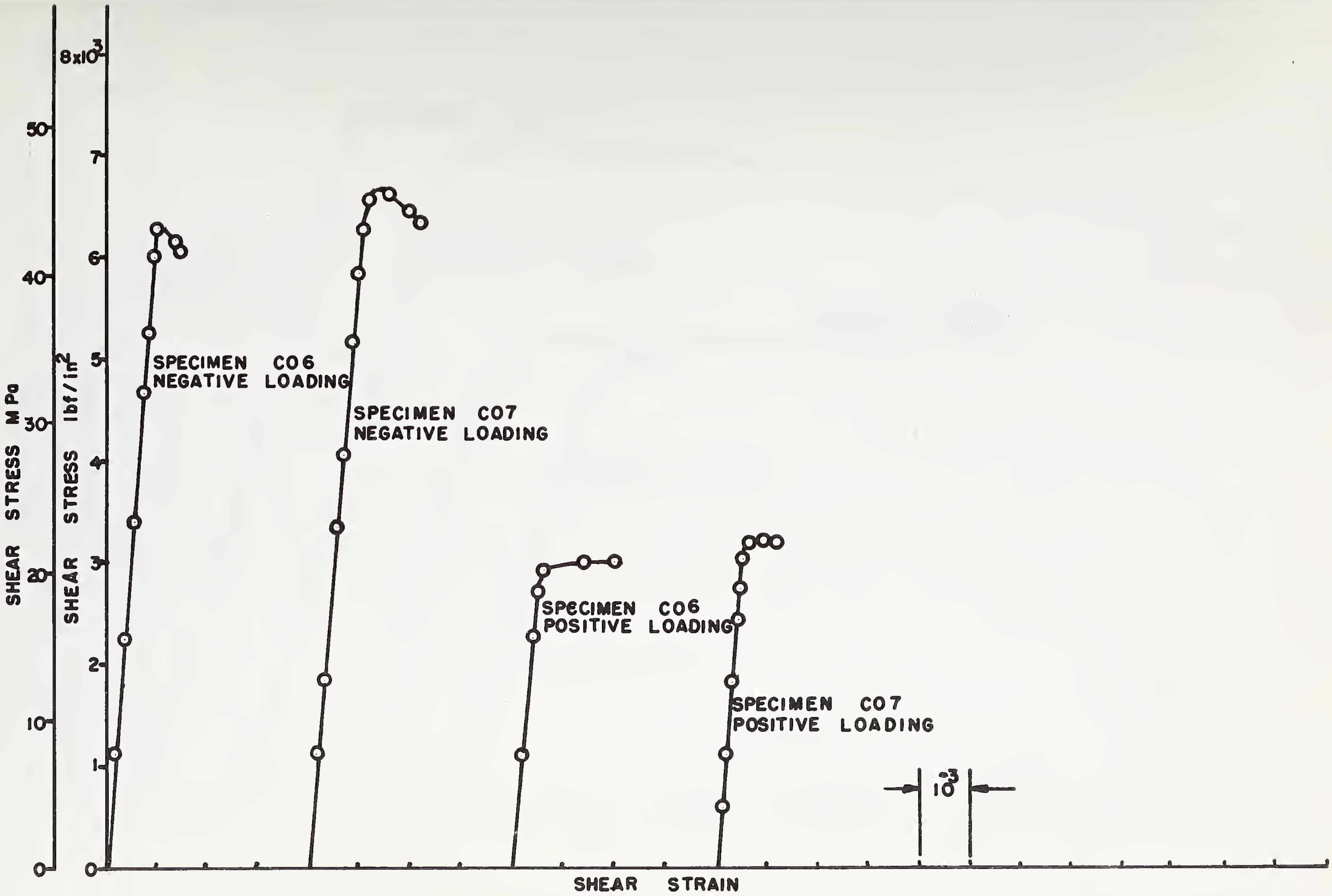

FIG. 7h— SHEAR STRESS— SHEAR STRAIN CURVES FOR SPECIMENS SHOWING EFFECTS OF STACKING SEQUENCE

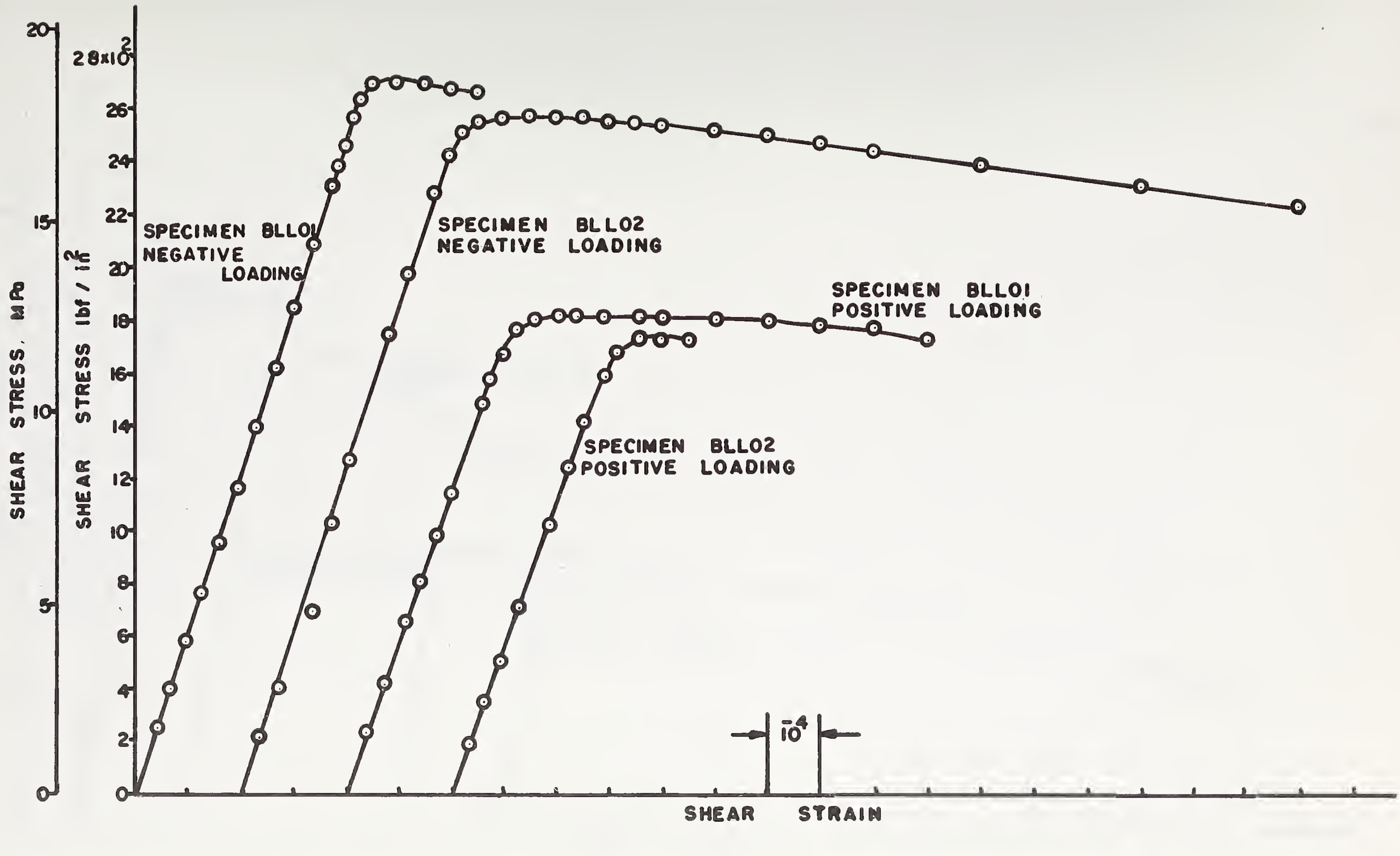

FIG. 7i – SHEAR STRESS – SHEAR STRAIN CURVES FOR SPECIMENS SHOWING EFFECTS OF LINEAR SCALING

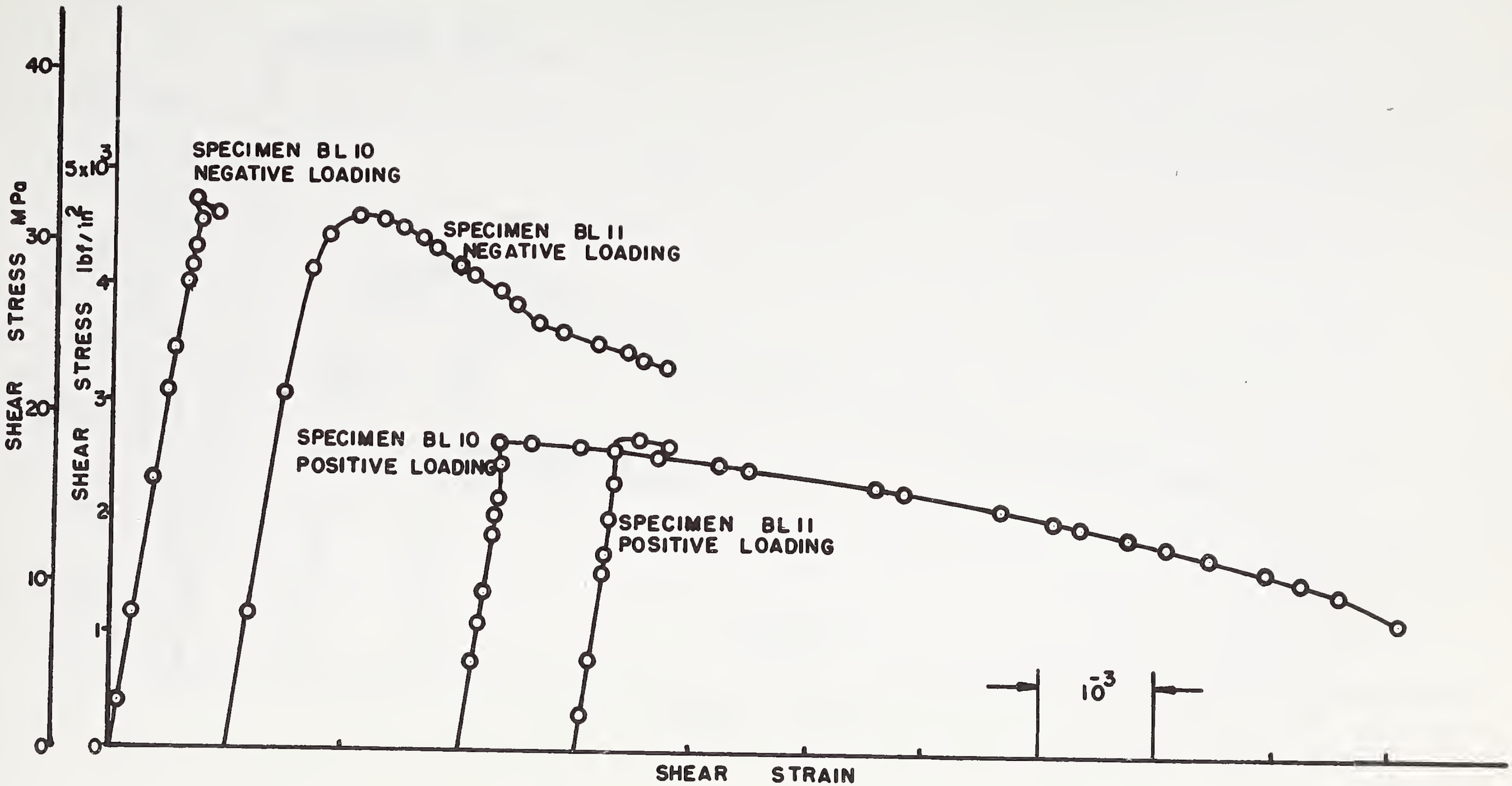

FIG. 7j — SHEAR STRESS — SHEAR STRAIN CURVES FOR SPECIMENS SHOWING EFFECTS OF LINEAR SCALING.

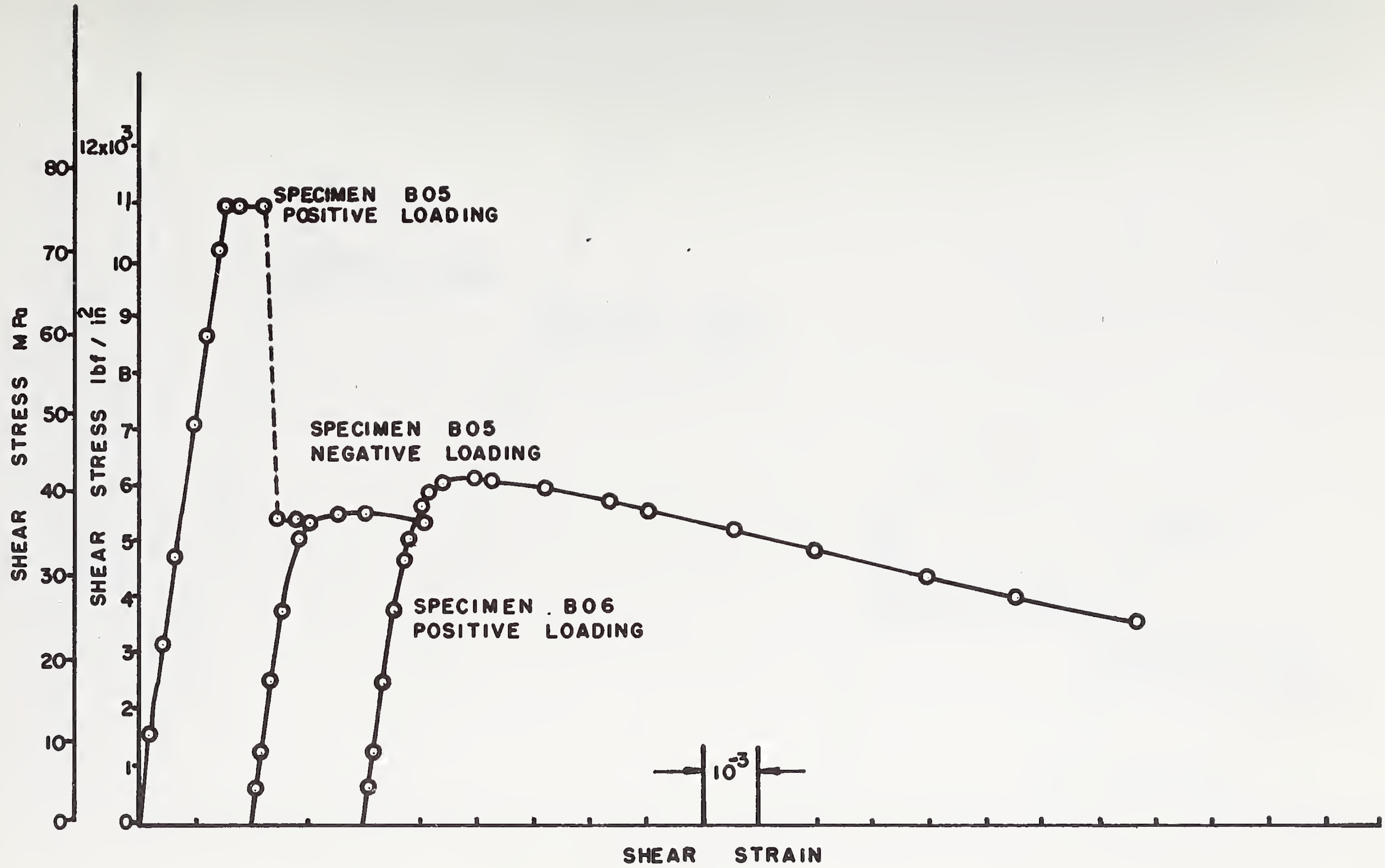

FIG. 7k.– SHEAR STRESS – SHEAR STRAIN CURVES FOR SPECIMENS SHOWING EFFECTS OF LINEAR SCALING

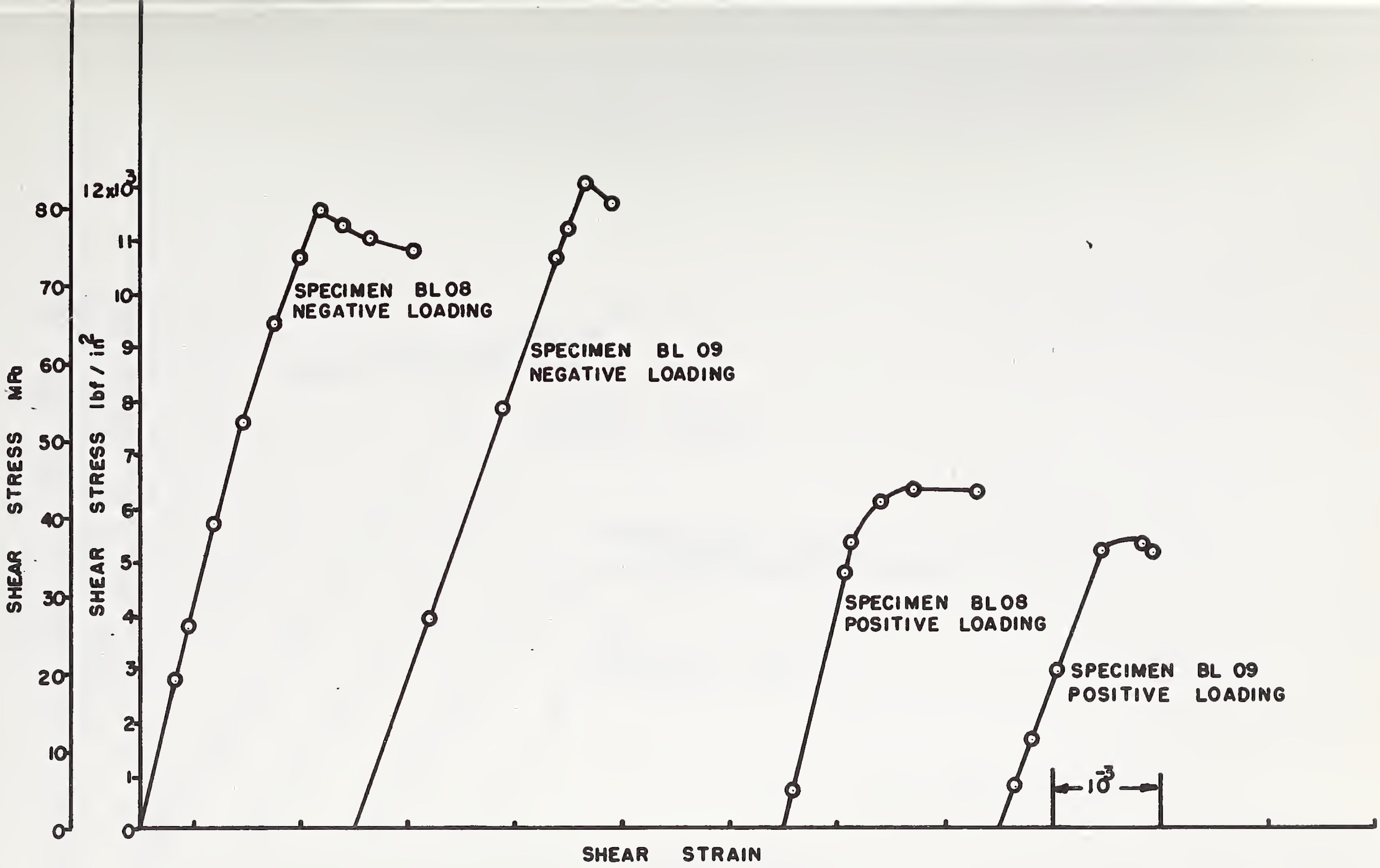

FIG. 71 - SHEAR STRESS—SHEAR STRAIN CURVES FOR SPECIMENS SHOWING EFFECTS OF LINEAR SCALING

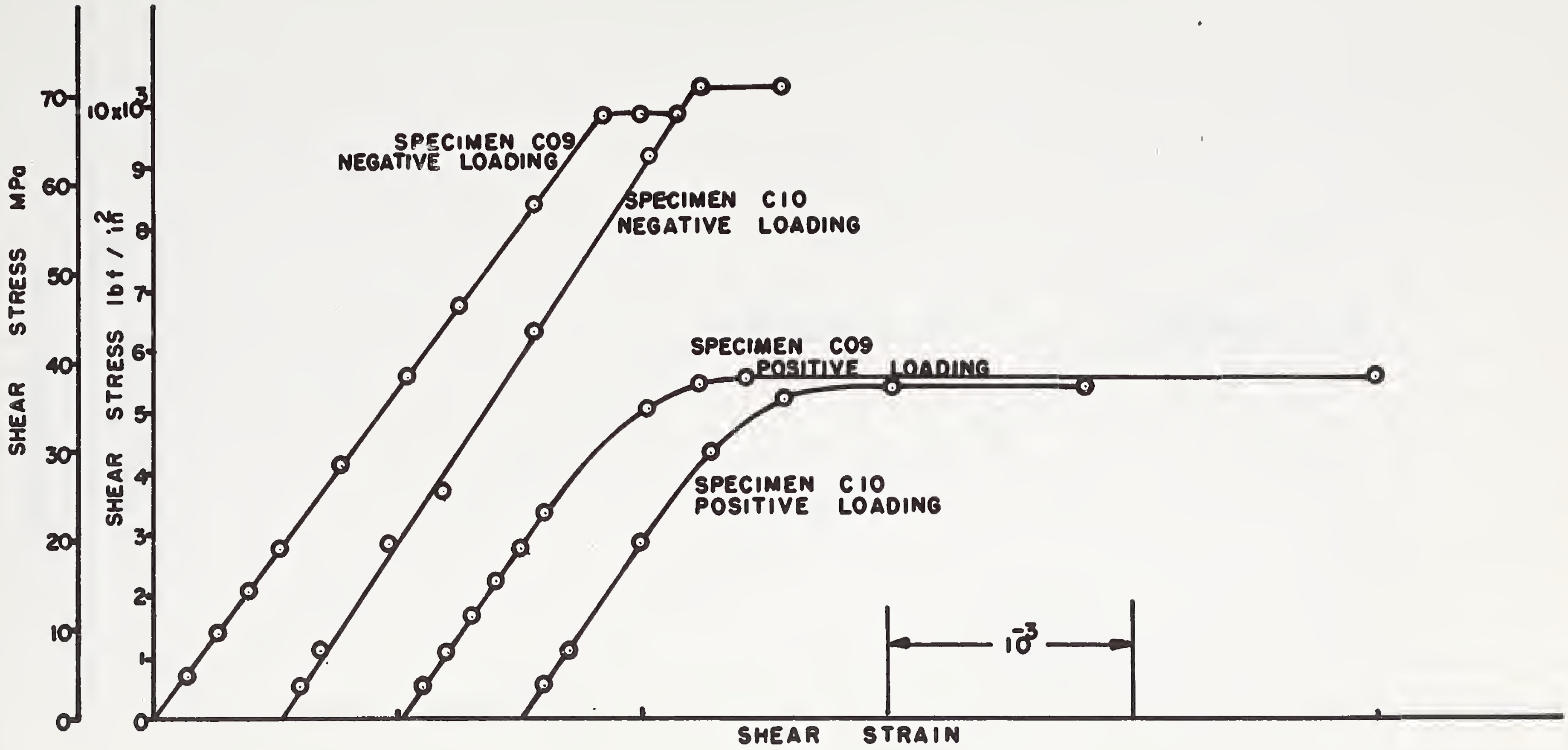

FIG. 7m— SHEAR STRESS–SHEAR STRAIN CURVES FOR SPECIMENS SHOWING EFFECTS OF LINEAR SCALING

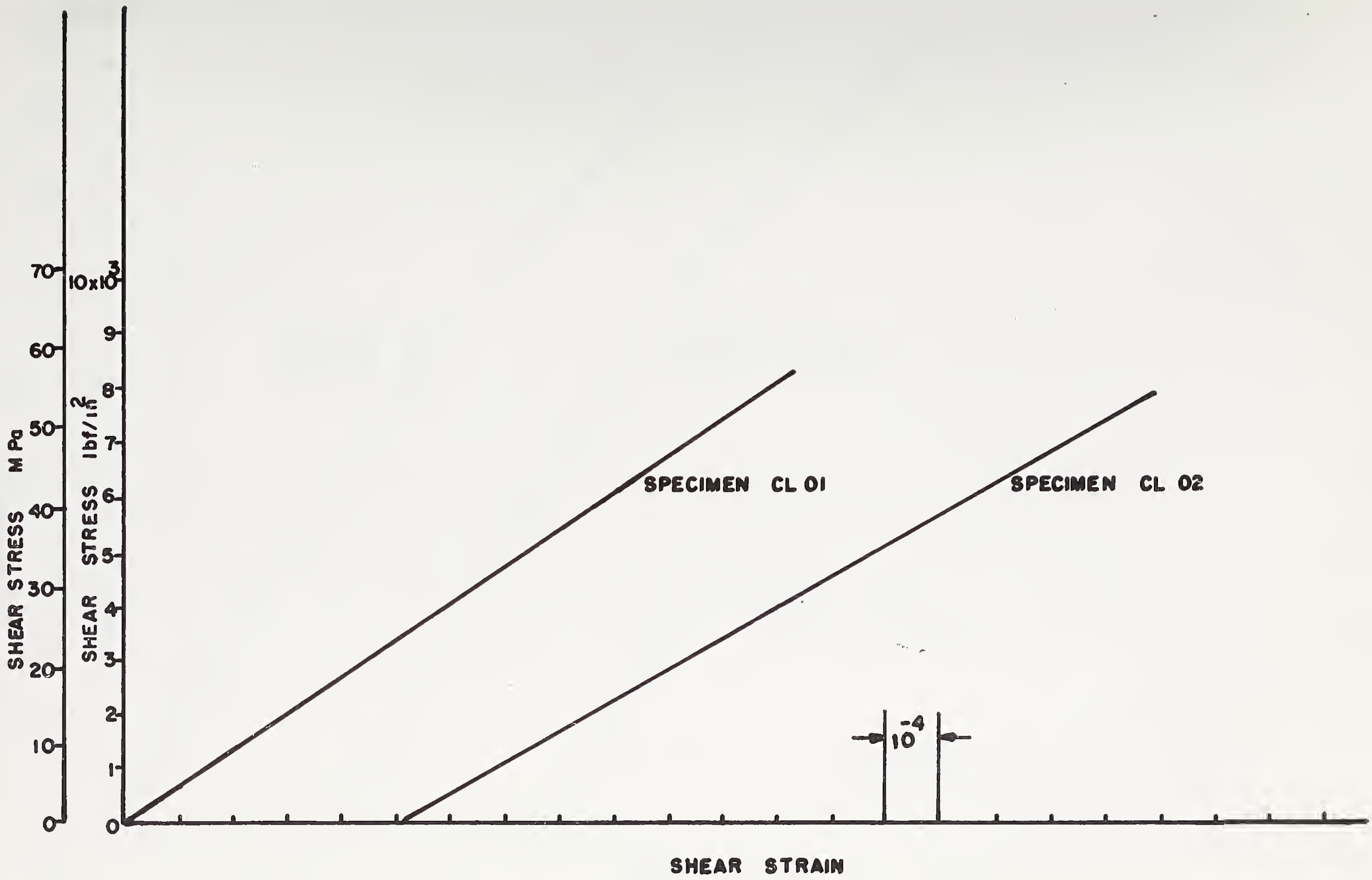

FIG. 7n— SHEAR STRESS—SHEAR STRAIN CURVES FOR SPECIMENS SHOWING EFFECTS OF LINEAR SCALING

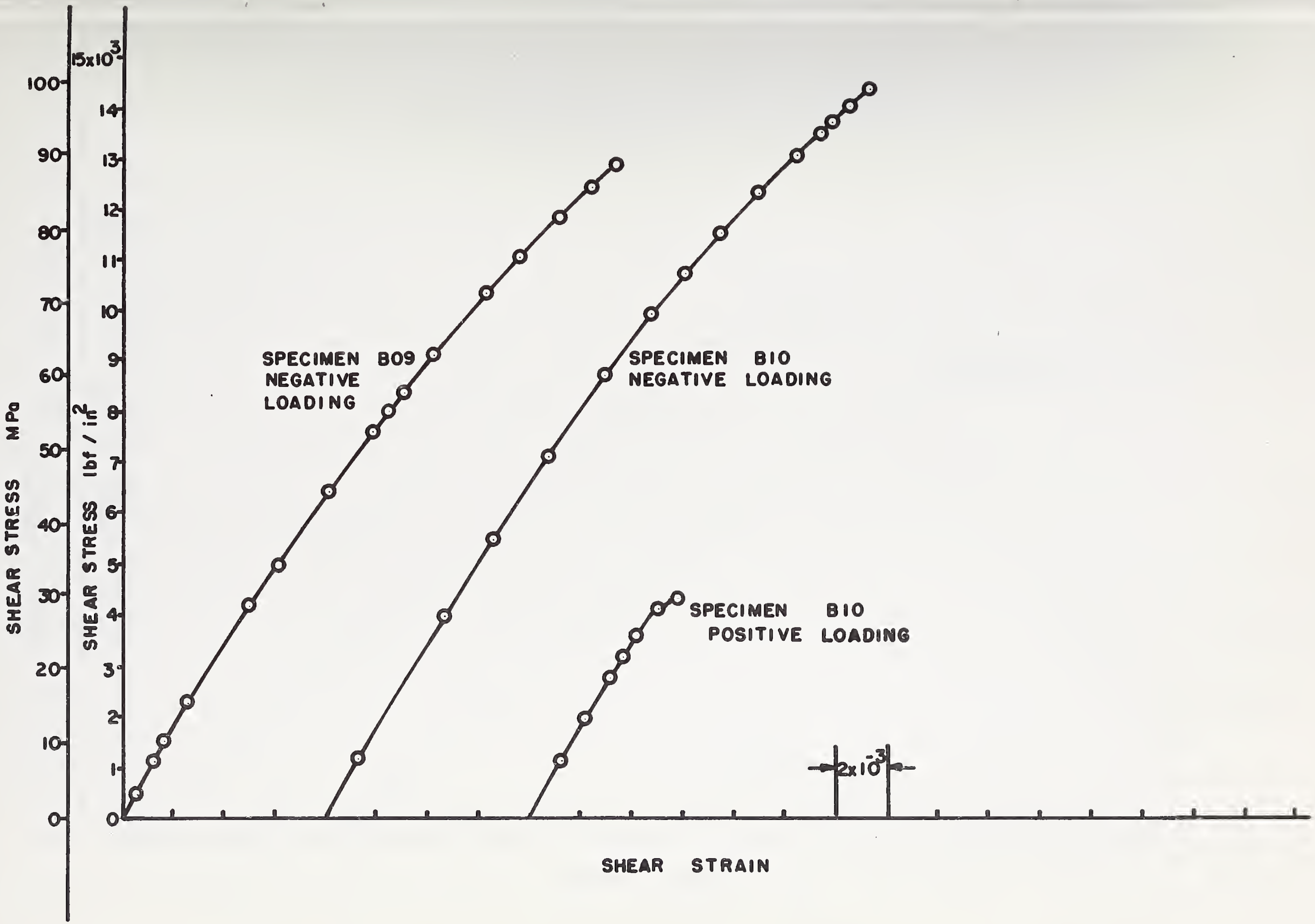

FIG. 7o SHEAR STRESS — SHEAR STRAIN CURVES FOR OPTIMUM ANGLE SPECIMENS

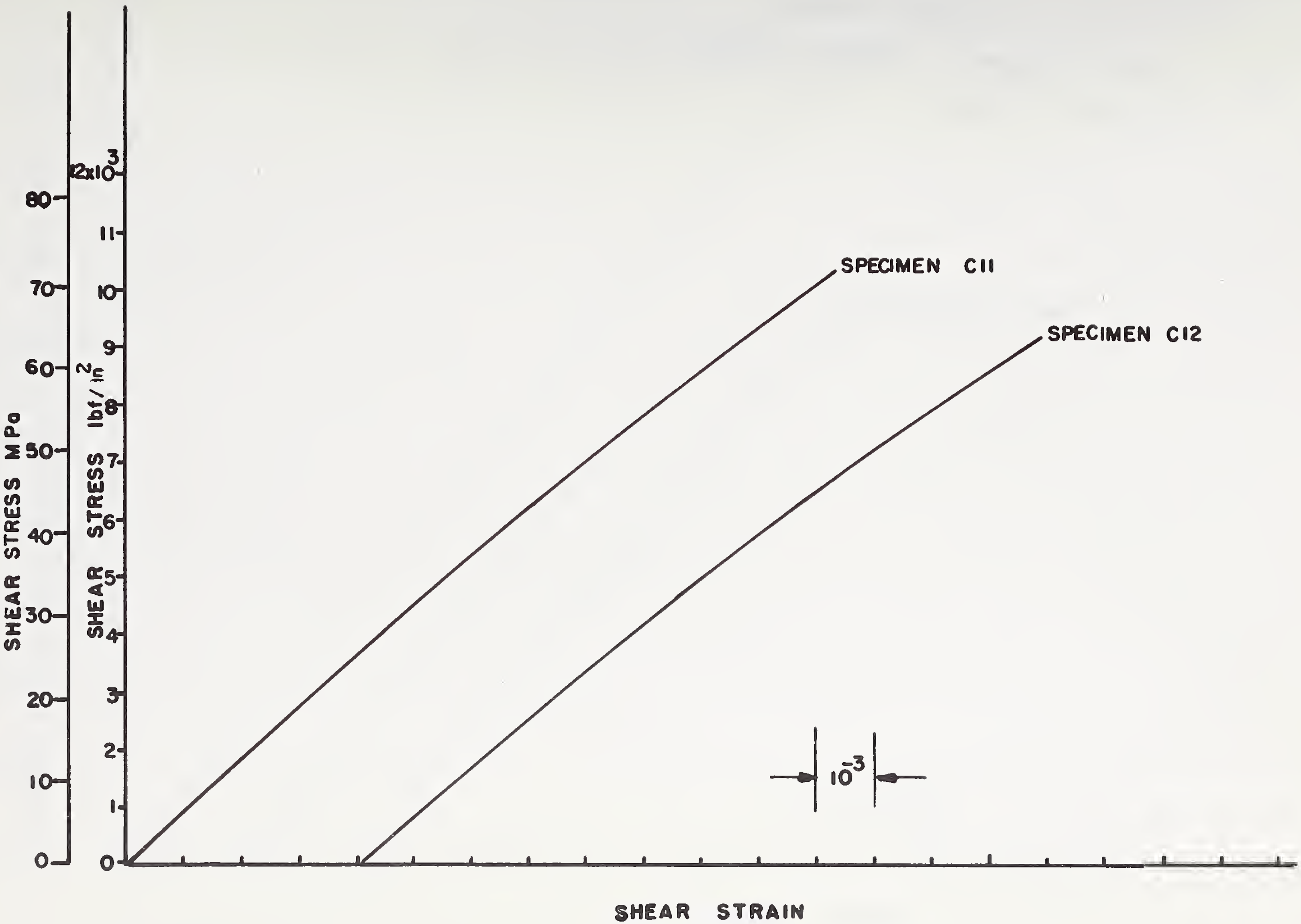

FIG. 7p – SHEAR STRESS–SHEAR STRAIN CURVES FOR "OPTIMUM" ANGLE SPECIMENS

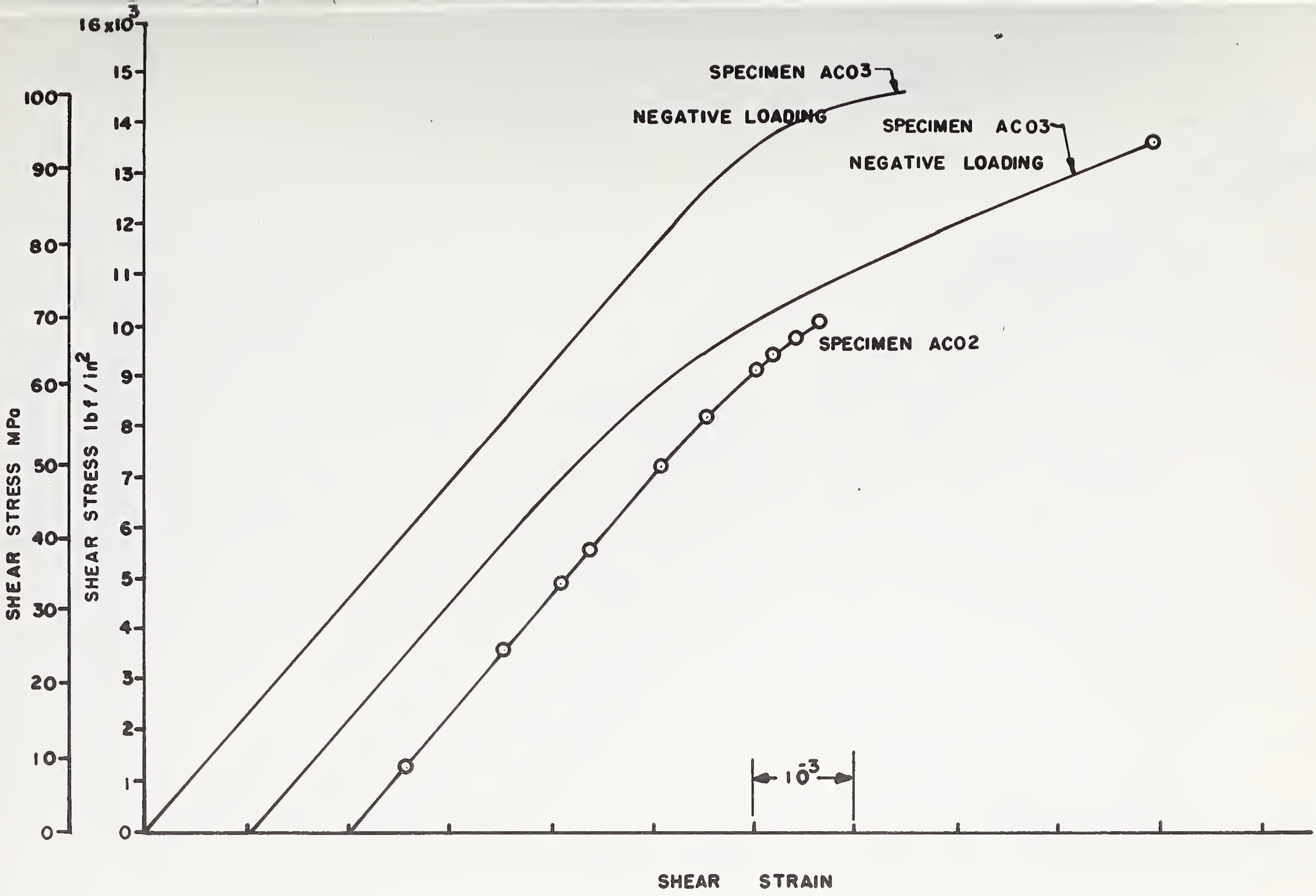

FIG. 7q—SHEAR STRESS—SHEAR STRAIN CURVES FOR COMPOSITE REINFORCED METAL SPECIMENS

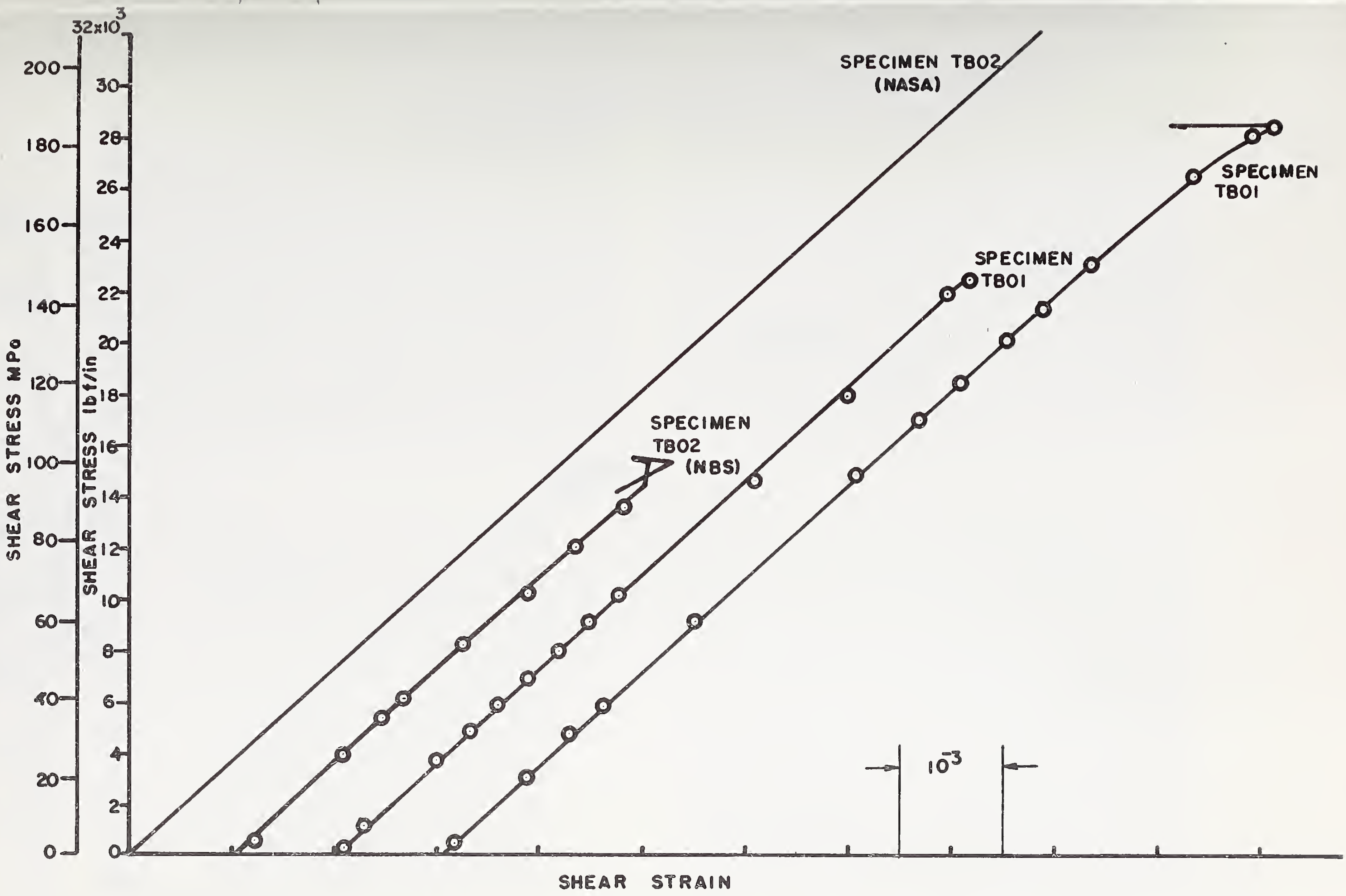

FIG. 7r – SHEAR STRESS–SHEAR STRAIN CURVES FOR COMPOSITE REINFORCED METAL SPECIMENS

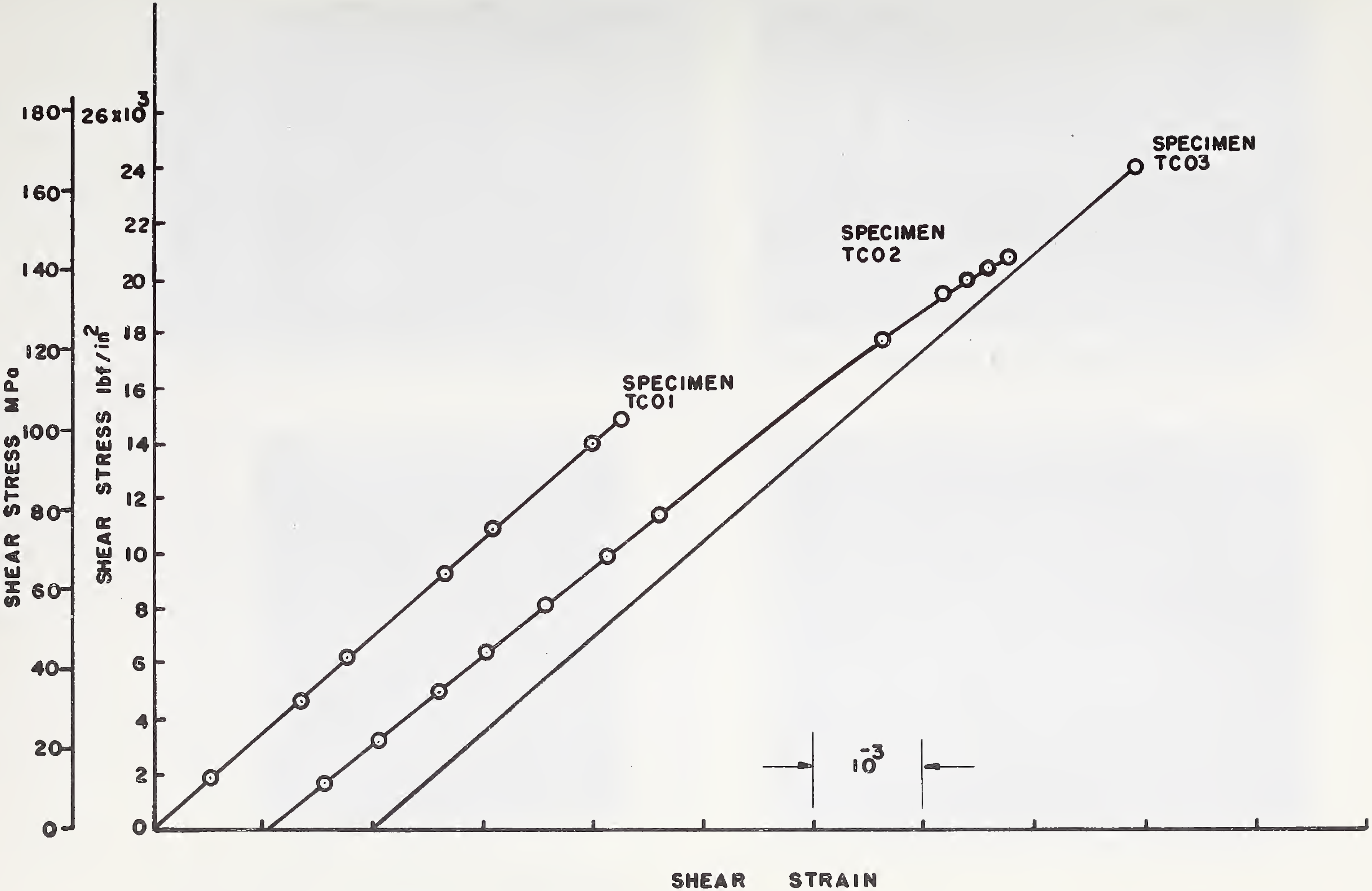

FIG. 7s -SHEAR STRESS-SHEAR STRAIN CURVES FOR COMPOSITE REINFORCED METAL SPECIMENS

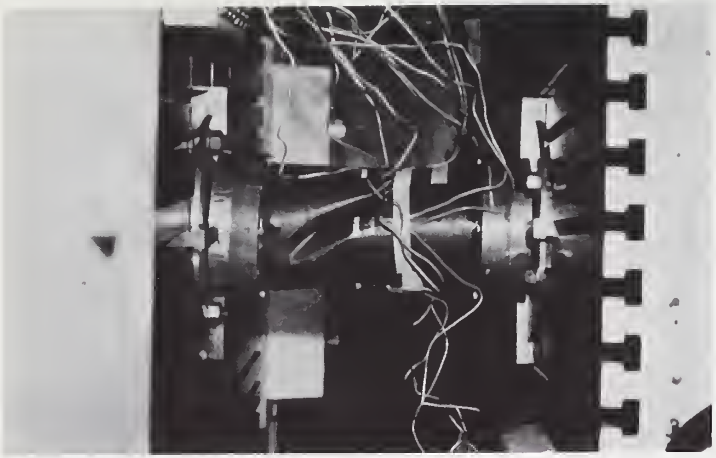

FIG. 8a SPECIMEN TBO2 LOADED NEGATIVE

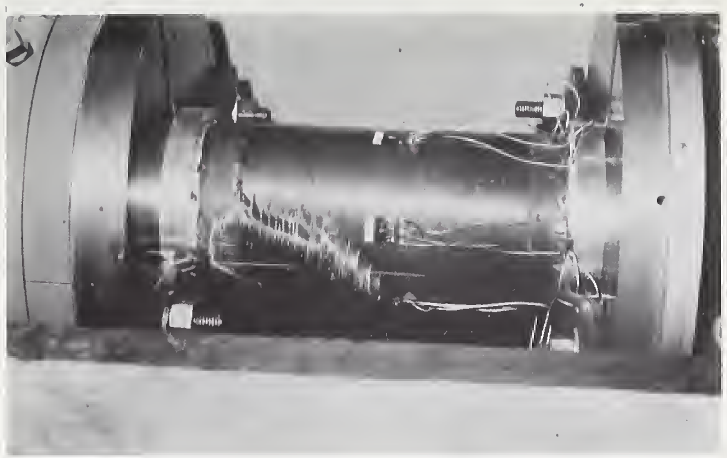

FIG. 8b SPECIMEN B10 LOADED NEGATIVE

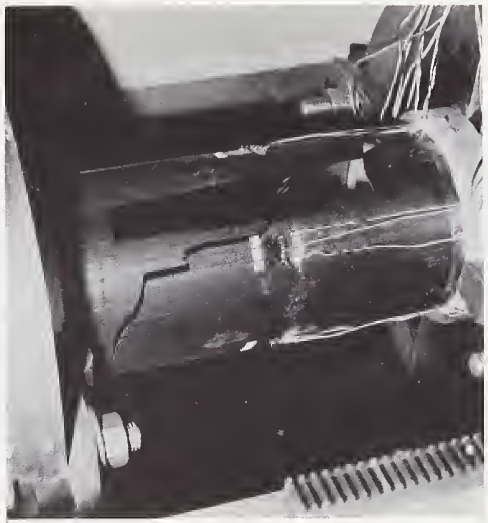

FIG. 8c SPECIMEN CO5

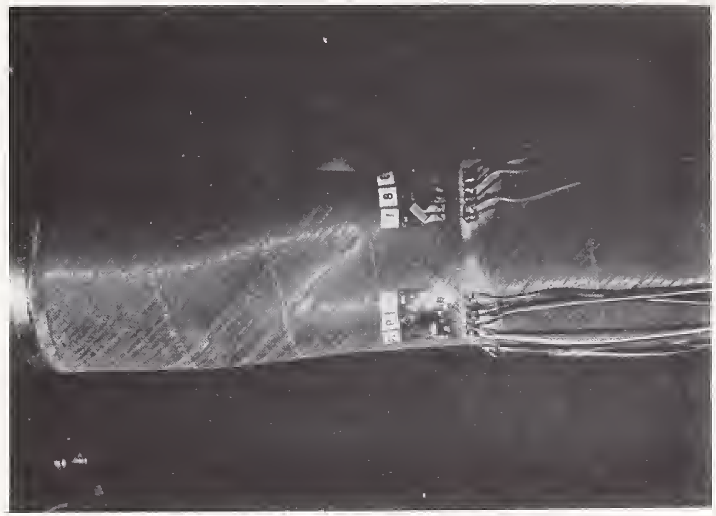

FIG. 8d SPECIMEN BO6 LOADED NEGATIVE

FIG. 8 TYPICAL BUCKLED SPECIMENS

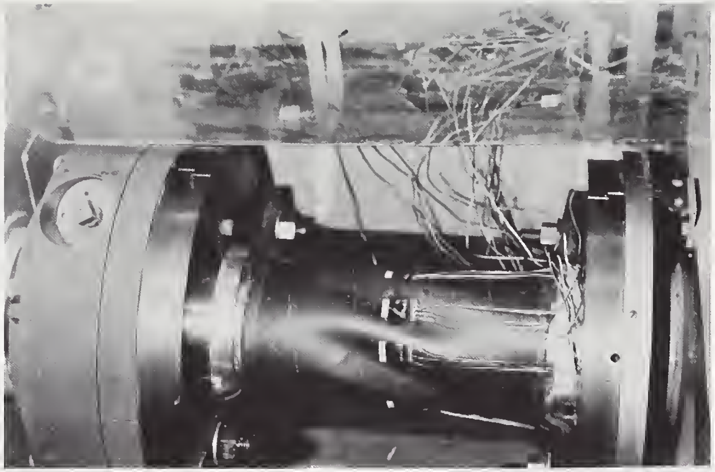
FIG. 8e SPECIMEN BO3 LOADED NEGATIVE

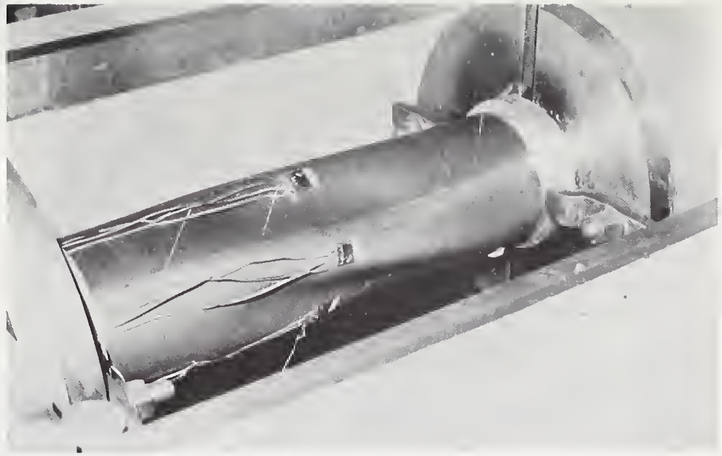
FIG. 8f SPECIMEN BL11 LOADED NEGATIVE

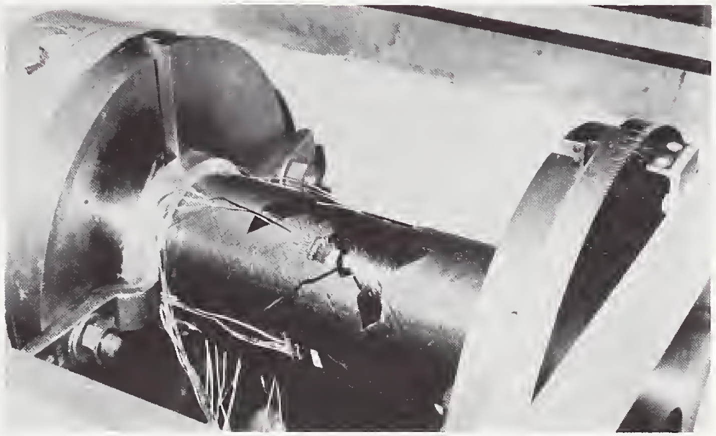
FIG. 8g SPECIMEN CO7 LOADED NEGATIVE

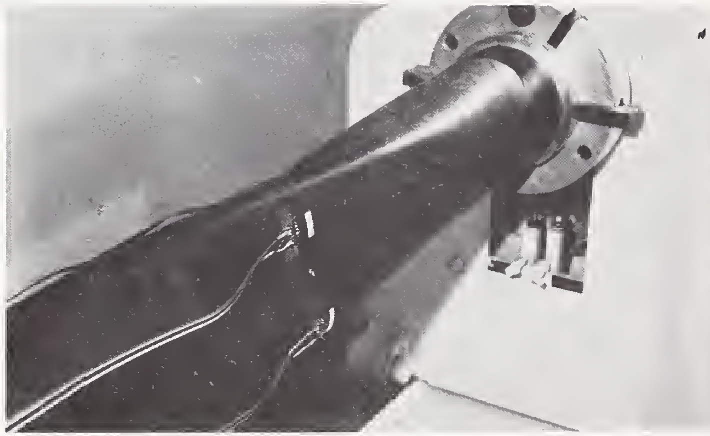
FIG. 8h SPECIMEN BLLO2 LOADED NEGATIVE

FIG. 8 TYPICAL BUCKLED SPECIMENS

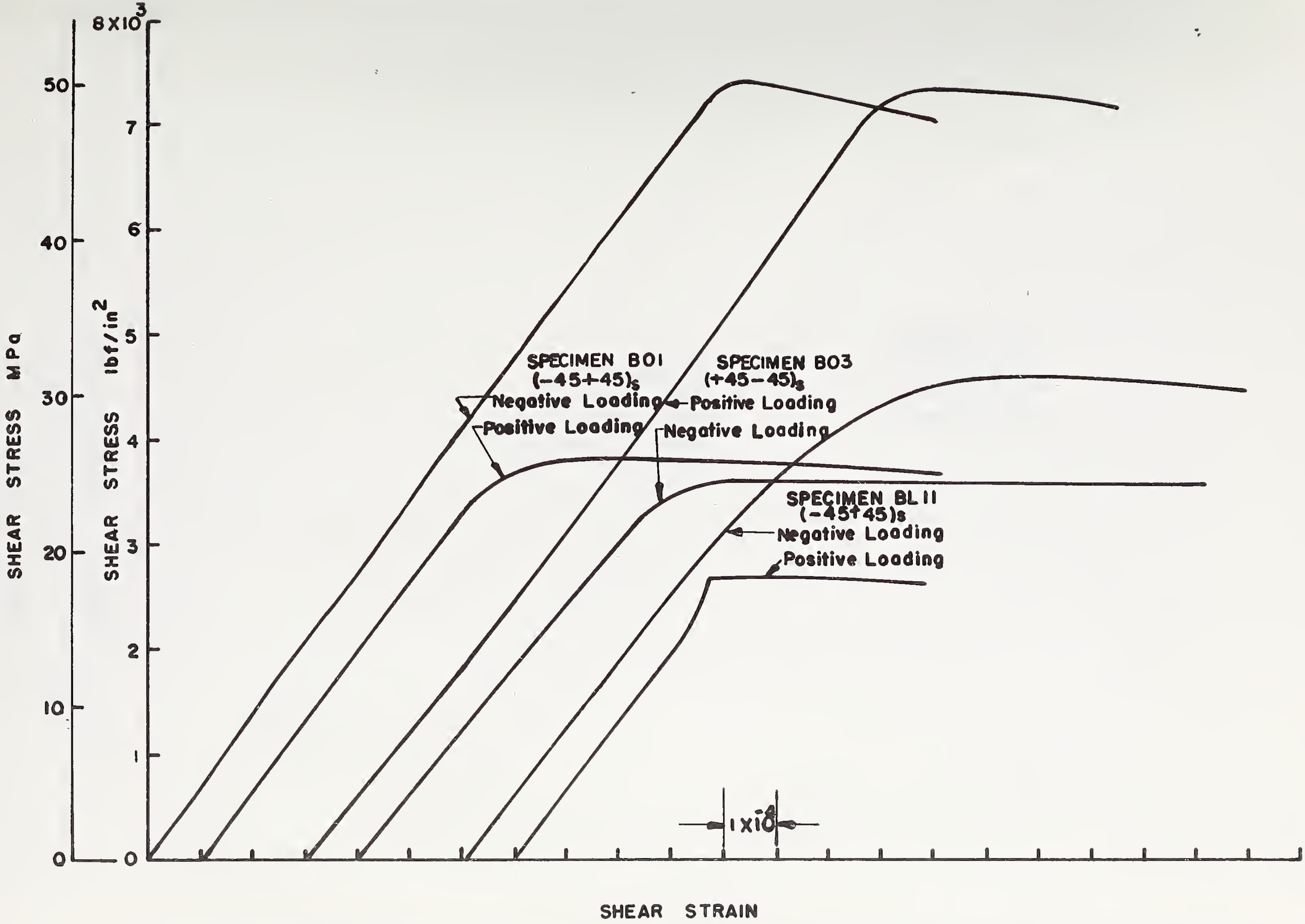

FIG. 9—SHEAR STRESS—SHEAR STRAIN CURVES SHOWING EFFECT OF REVERSING LOADING AND STACKING SEQUENCE FOR BORON/EPOXY SPECIMENS

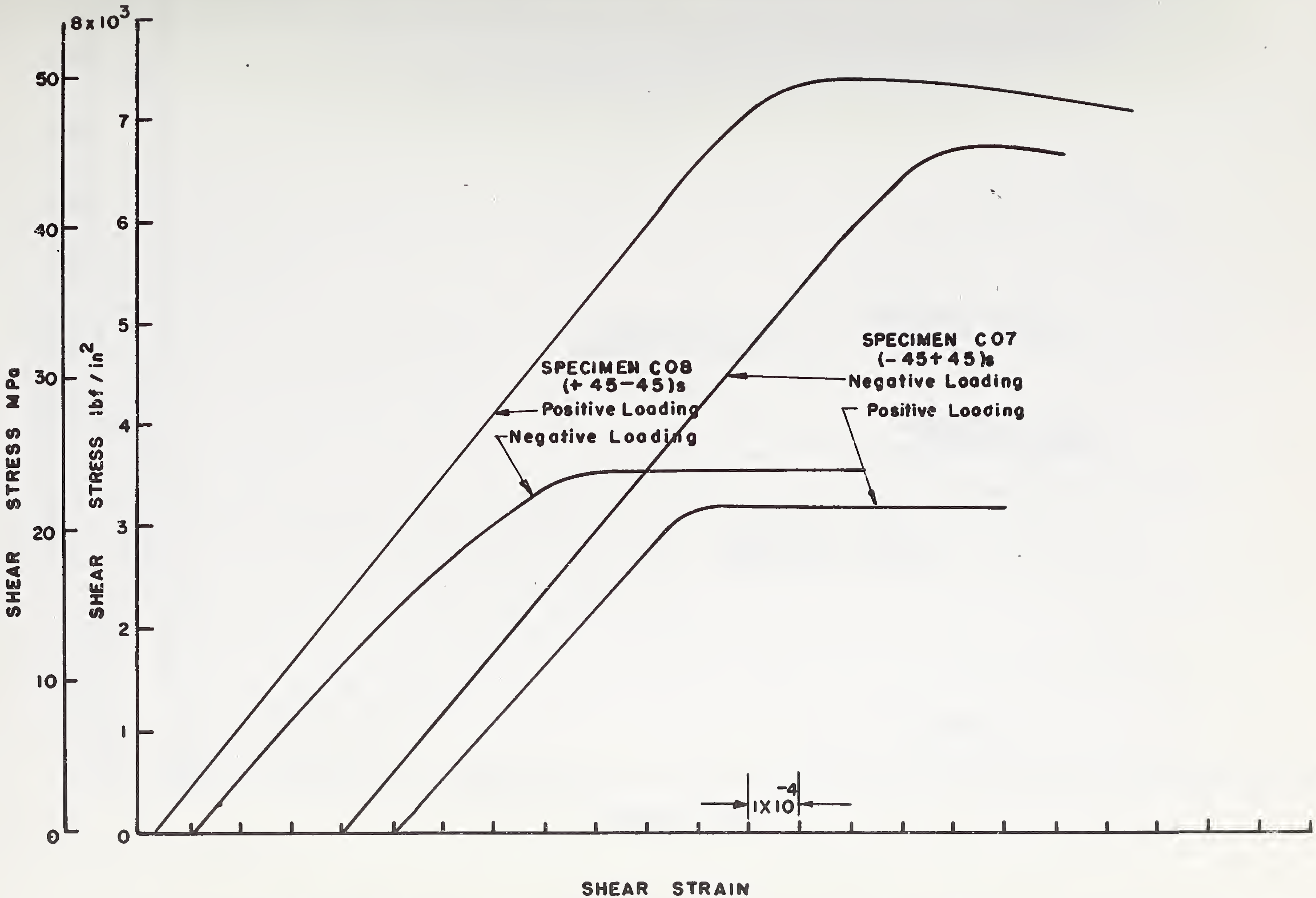

FIG. 10— SHEAR STRESS—SHEAR STRAIN CURVES SHOWING EFFECT OF REVERSING LOADING AND STACKING SEQUENCE FOR GRAPHITE/EPOXY SPECIMENS

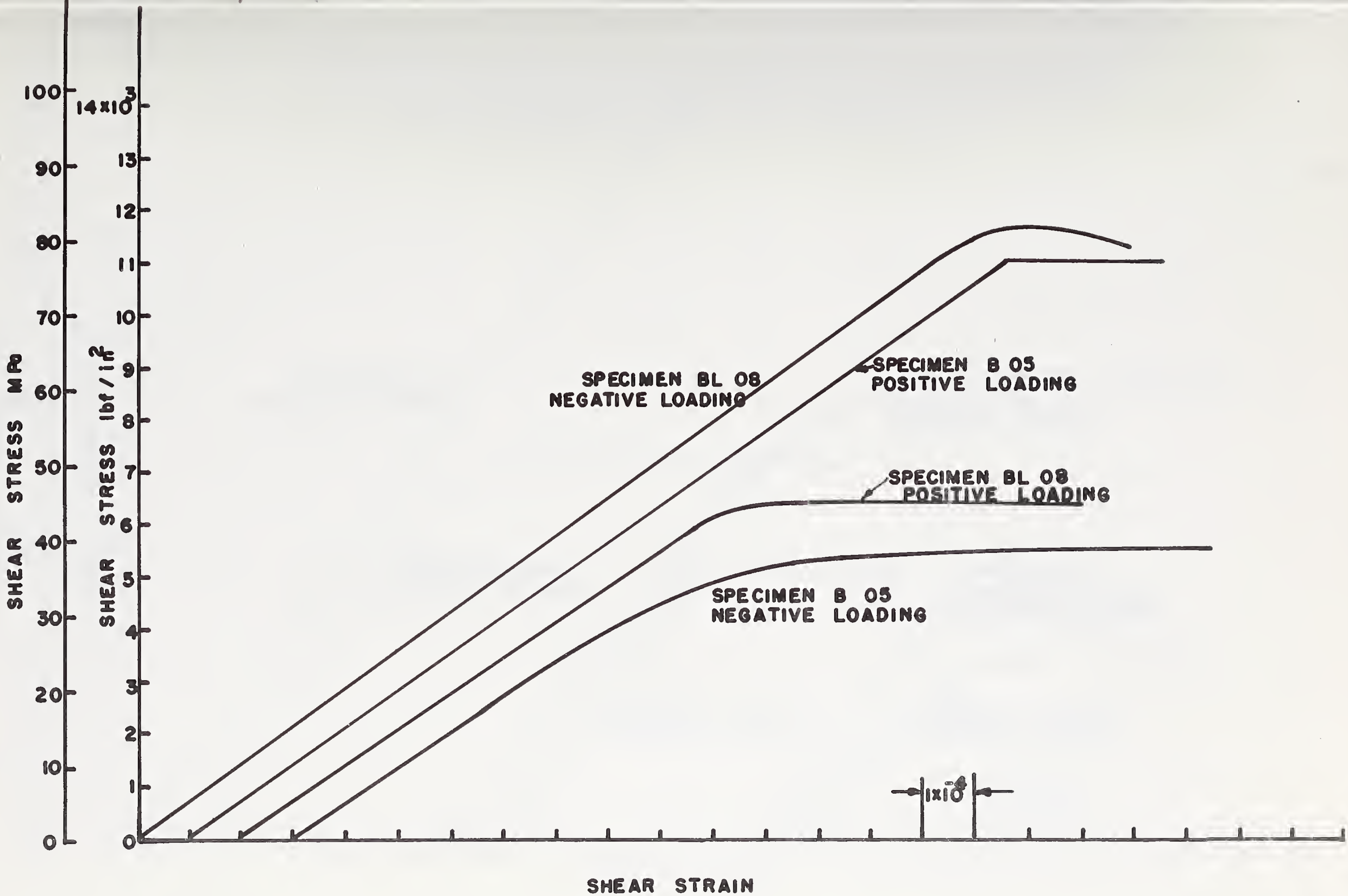

FIG. 11—SHEAR STRESS—SHEAR STRAIN CURVE SHOWING EFFECT OF LINEAR SCALING OF TUBE DIMENSIONS FOR BORON / EPOXY CYLINDERS

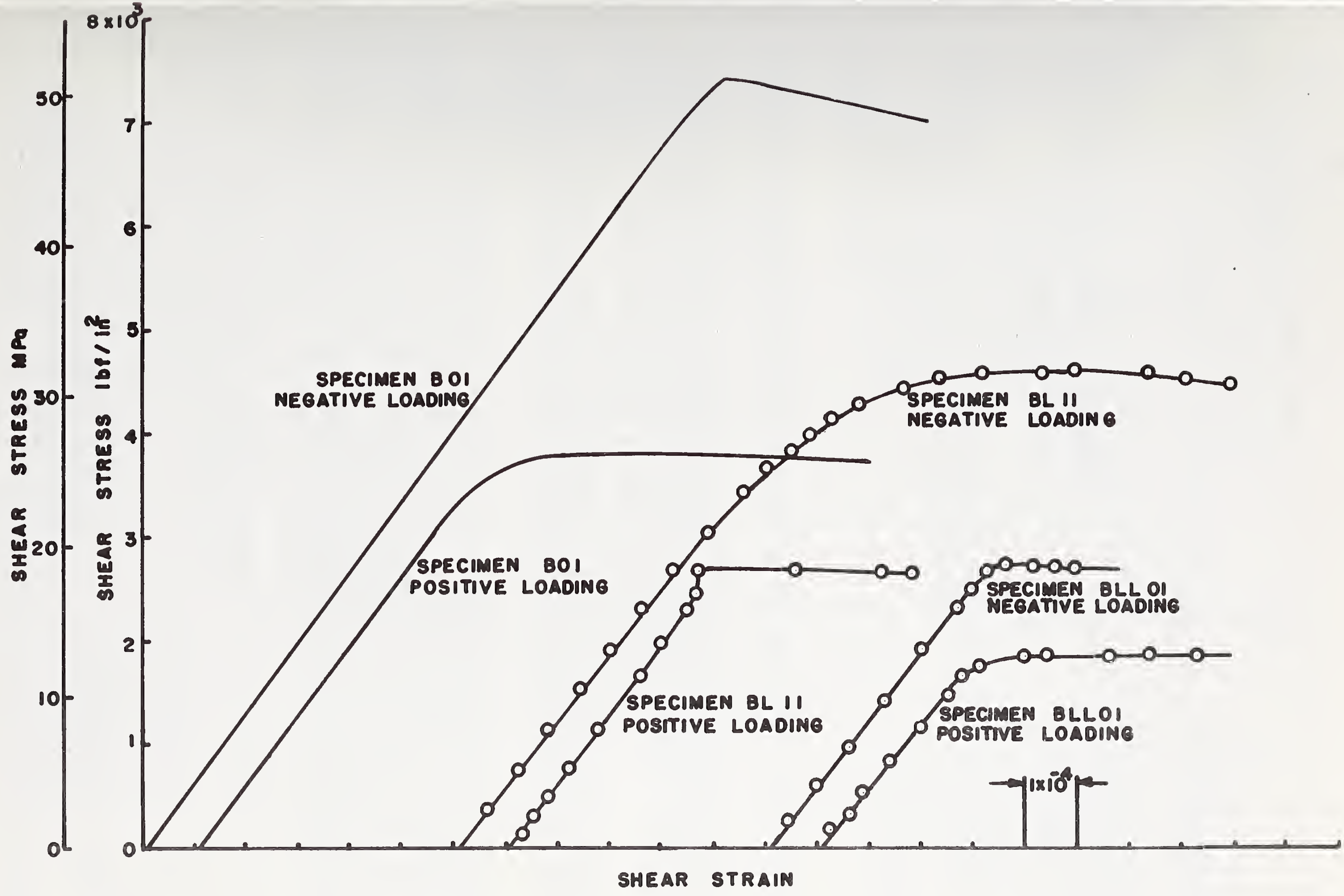

FIG. 12—SHEAR STRESS—SHEAR STRAIN CURVE SHOWING EFFECT OF SCALING OF SPECIMEN LENGTH FOR BORON EPOXY CYLINDERS

NBS-114A (REV. 7-73)

U.S. DEPT. OF COMM. BIBLIOGRAPHIC DATA SHEET	1. PUBLICATION OR REPORT NO. NBSIR 74-572	2. Gov't Accession No.	3. Recipient's Accession No.

4. TITLE AND SUBTITLE

Torsional Buckling of Composite Cylindrical Shells

5. Publication Date September 1974

6. Performing Organization Code

7. AUTHOR(S)

D. E. Marlowe and G. F. Sushinsky

8. Performing Organ. Report No. NBSIR 74-572

9. PERFORMING ORGANIZATION NAME AND ADDRESS

NATIONAL BUREAU OF STANDARDS
DEPARTMENT OF COMMERCE
WASHINGTON, D.C. 20234

10. Project/Task/Work Unit No. 2130445

11. Contract/Grant No. L-48, 826

12. Sponsoring Organization Name and Complete Address *(Street, City, State, ZIP)*

National Aeronautics and Space Administration
Langley Research Center
Hampton, Virginia 23365

13. Type of Report & Period Covered Final

14. Sponsoring Agency Code

15. SUPPLEMENTARY NOTES

16. ABSTRACT *(A 200-word or less factual summary of most significant information. If document includes a significant bibliography or literature survey, mention it here.)*

The elastic buckling strength has been determined for thin-walled composite and composite-reinforced-metal cylindrical shells. Tests were performed on boron/epoxy and graphite/epoxy-all-composite specimens, on boron/epoxy-reinforced-titanium specimens and on boron/epoxy and graphite/epoxy-reinforced aluminum specimens. Cylinders were tested with several unidirectional-ply and cross-ply layups.

The results of the tests were compared with the buckling strengths predicted by the torsional buckling analysis of Chao. For the cylinders which fail by buckling, the experimental buckling torques were approximately 81 percent of the torques predicted by the analysis.

The experimental results of tests on 39 specimens are presented. Torsional buckling strengths which differ by as much as a factor of two may result from reversing the direction of twist of a thin-walled cross-ply composite cylinder. This has been shown to be equivalent to reversing the stacking sequence of the laminate. This is of potential importance in applications where reversals of loading may occur. An "optimum" stacking sequence which produced significant increases in the predicted and measured buckling loads was determined. Cylinders fabricated with this stacking sequence exhibit considerable increases in the strength-to-weight ratio over other sequences examined.

17. KEY WORDS *(six to twelve entries; alphabetical order; capitalize only the first letter of the first key word unless a proper name; separated by semicolons)*

Aircraft structures; buckling; composite materials; metal reinforcement; stability; stacking sequence; thin shells; torsion.

18. AVAILABILITY [X] Unlimited

[ ] For Official Distribution. Do Not Release to NTIS

[ ] Order From Sup. of Doc., U.S. Government Printing Office Washington, D.C. 20402, SD Cat. No. C13

[ ] Order From National Technical Information Service (NTIS) Springfield, Virginia 22151

19. SECURITY CLASS (THIS REPORT) UNCLASSIFIED

20. SECURITY CLASS (THIS PAGE) UNCLASSIFIED

21. NO. OF PAGES 65

22. Price

USCOMM-DC 29042-P74